Design of an Electrothermally Actuated SU-8 based Microgripper for Biomedical Applications

Author

MUHAMMAD ZAEEM ABBAS

00000119954

Supervisor

DR. MUHAMMAD MUBASHER SALEEM

DEPARTMENT OF MECHATRONICS ENGINEERING

COLLEGE OF ELECTRICAL & MECHANICAL ENGINEERING

NATIONAL UNIVERSITY OF SCIENCES AND TECHNOLOGY

ISLAMABAD

JULY, 2018

Design of an Electrothermally Actuated SU-8 based Microgripper for Biomedical Applications

Author

MUHAMMAD ZAEEM ABBAS

00000119954

A thesis submitted in partial fulfillment of the requirements for the degree of

MS Mechatronics Engineering

Thesis Supervisor:

DR. MUHAMMAD MUBASHER SALEEM

Thesis Supervisor's Signature: ____

DEPARTMENT OF MECHATRONICS ENGINEERING

COLLEGE OF ELECTRICAL & MECHANICAL ENGINEERING

NATIONAL UNIVERSITY OF SCIENCES AND TECHNOLOGY, ISLAMABAD

JULY, 2018

Declaration

I certify that this research work titled "*Design of an Electrothermally Actuated SU-8 based Microgripper for Biomedical Applications"* is my own work. The work has not been presented elsewhere for assessment. The material that has been used from other sources it has been properly acknowledged / referred.

Signature of Student

Muhammad Zaeem Abbas

00000119954

Language Correctness Certificate

This thesis has been read by an English expert and is free of typing, syntax, semantic, grammatical and spelling mistakes. Thesis is also according to the format given by the university.

Signature of Student

Muhammad Zaeem Abbas

00000119954

Signature of Supervisor

Dr. Muhammad Mubasher Saleem

Copyright Statement

- Copyright in text of this thesis rests with the student author. Copies (by any process) either in full, or of extracts, may be made only in accordance with instructions given by the author and lodged in the Library of NUST College of E&ME. Details may be obtained by the Librarian. This page must form part of any such copies made. Further copies (by any process) may not be made without the permission (in writing) of the author.
- The ownership of any intellectual property rights which may be described in this thesis is vested in NUST College of E&ME, subject to any prior agreement to the contrary, and may not be made available for use by third parties without the written permission of the College of E&ME, which will prescribe the terms and conditions of any such agreement.
- Further information on the conditions under which disclosures and exploitation may take place is available from the Library of NUST College of E&ME, Rawalpindi.

Acknowledgements

In the name of Allah, the Most Gracious and the Most Merciful. Alhamdulillah, all praises to Allah for the strengths and His blessing in completing this thesis. I am very grateful to my Creator Allah Subhana-Watala to have guided me throughout my life and in this work at every step and for every new thought, which You create in my mind to improve it. Indeed, I could have done nothing without Your priceless help and guidance.

I am profusely thankful to my beloved parents and family who raised me when I was not capable of walking and continued to support me morally and financially throughout in every department of my life. Whatever I am today, is due to their prayers.

I would also like to express special thanks to my supervisor Dr. Muhammad Mubasher Saleem for his help throughout my thesis and for Microelectromechanical Systems course, which he has taught me. I can safely say that I haven't learned any other engineering subject in such depth than the one which he has taught. Dr. Muhammad Mubasher Saleem showed personal interest, tremendous support and cooperation in this thesis. He personally monitored me during experimentation phase. He consistently allowed this thesis to be my own work, but steered me in the right the direction whenever he thought I needed it. Each time I got stuck in something, he came up with the solution. Without his help I wouldn’t have been able to complete my thesis. I appreciate his patience and guidance throughout the whole thesis. I can easily say that he is more than teacher and mentor for me.

I would also like to thank Dr. Umar Shahbaz Khan and Dr. Mohsin Islam Tiwana for guiding me through thesis and evaluation committee. I would like to thank and acknowledge the efforts of Muhammad Umar Masood for his help during thesis. I would also like to express my special thanks to my classmates Muhammad Fahad Sheikh, Muhammad Arslan, Ubaid-Ur-Rehman, Nabeel-Ur-Rehman, Muhammad Altaph, and Osama bin Islam for their support.

Finally, I would like to express my gratitude to all the individuals who have rendered valuable assistance to my study.

Dedicated to my parents and my sisters for their constant support

Abstract

For a past few decades, micro manipulation has become a significant task in the fields of microelectromechanical systems, cell biology and cell mechanics. To study cell mechanics and cell biology, sample are required. Previously, micropipetes were used to take biological samples in bulk. Optical tweezers were also used for isolating particles and objects with dimensions in microns. Now a day, these samples are taken with the help of a microgripper.

In this work, a biocompatible microgripper design is presented for cell manipulation of multiple size. Microgripper is a MEMS device, commonly named as microtweezer, micrograsper and micromanipulator. It is a device that can grip, hold, relocate, rotate, pick and place objects with dimensions in microns. Objects include from components of microrobots to a living cell of various shape and size. This wide range in size of living and non-living objects under observation, leads to the development of variety of microgrippers available today. This works targets the cell manipulation with wide gripping range at low power and compact in size.

Key Words: *Microgripper, Electrothermal actuator, Cell manipulation, Biomedical application*

Table of Contents

Declaration .... **i**
Language Correctness Certificate .... **ii**
Copyright Statement .... **iii**
Acknowledgements .... **iv**
Abstract .... **vi**
Table of Contents .... **vii**
List of Figures .... **ix**
List of Tables .... **x**
CHAPTER 1: INTRODUCTION **1**
1.1 Microgripper Applications 1
1.2 Microgrippers 1
1.3.1 Electrostatic Actuators 3
1.3.2 Piezoelectric Actuators 4
1.3.3 Electrothermal Actuators 5
1.3.4 Other Actuators 8
1.4 Microfabrication process 11
1.4.1 SOIMUMPs 11
1.4.2 MetalMUMPs 11
1.4.3 PolyMUMPs 11
1.4.4 LIGA process 12
1.4.5 Polymer based fabrication 12
1.4.6 Advantages of SU-8 12
CHAPTER 2: LITERATURE REVIEW **14**
2.1 Electrostatic Microgrippers 14
2.2 Piezoelectric Microgrippers 16
2.3 Electrothermal Microgrippers 18
CHAPTER 3: PROPOSED MICROGRIPPER DESIGN **24**
3.1 Electrothermal Actuator 25
3.2 Compliant Mechanisms 26
3.2.1 Scott Russell Mechanism 26
3.2.2 Multi-stage Compound Radial Flexure 28
3.2.3 Leverage Mechanism 29
3.3 Gripping Jaws 30

3.4 Mathematical Model of Proposed Microgripper Design 32
3.5 Results 42
CHAPTER 4: VERIFICATION OF MICROGRIPPER DESIGN 46
4.1 Finite Element Method 46
4.2 Initial Loading Conditions 46
4.3 Analysis Types 47
4.3.1 Thermal-Electric Analysis 48
4.3.2 Static Structural Analysis 50
4.4 Results 54
CHAPTER 5: DISCUSSION AND COMPARISON 58
5.1 Mathematical Model vs FEM Results 58
5.2 Discussion 60
5.3 Comparison 61
CHAPTER 6: CONCLUSION 62
REFERENCES 63

List of Figures

Figure 1.1: Electrostatic actuator types (a) Transverse Comb Drive Actuator [17], (b) Lateral Comb Drive Actuator [18] 3
Figure 1.2: Microgripper with piezoelectric actuator and leverage mechanism [7] 5
Figure 1.3: Electrothermal Chevron actuator configurations (a) series configuration [25], (b) parallel configuration [24] 6
Figure 1.4: Bimorph electrothermal actuator [22] 6
Figure 1.5: U-shaped electrothermal Actuator [23] 7
Figure 1.6: Microgripper made of SMA [31] 8
Figure 1.7: IPMC actuator (a) deactivated state, (b) actuated state [32] 9
Figure 1.8: Hydraulic Actuator [33] 9
Figure 1.9: Pneumatically actuated microgripper (a) microgripper, (b) actuator [34] 10
Figure 1.10: VCM based microgripper (a) actuated state, (b) deactivated state [35] 10
Figure 3.1: Proposed microgripper design with various components mentioned 24
Figure 3.2: Design of actuator with annotations 26
Figure 3.3: Cross-section of actuator with annotations 26
Figure 3.4: Scott Russell mechanism working principle with annotations 27
Figure 3.5: Scott Russell mechanism with annotations 28
Figure 3.6: Multi-stage Compound Radial Flexure mechanism with annotations 29
Figure 3.7: Leverage mechanism working principle and annotations 30
Figure 3.8: Microgripper Jaw 32
Figure 3.9: Voltage vs displacement graph from mathematical model 43
Figure 3.10: Voltage vs average change in temperature graph from mathematical model 43
Figure 3.11: Power vs displacement graph from mathematical model 44
Figure 3.12: External force vs displacement graph from mathematical model 45
Figure 4.1: Front facing view of mesh of important components of the microgripper 47
Figure 4.2: Current Density profile through gold heater in actuator 48
Figure 4.3: Temperature profile of complete microgripper 49
Figure 4.4: Displacement in X-axis direction 50
Figure 4.5: Displacement in Y-axis direction 51
Figure 4.6: Displacement in Z-axis direction 52
Figure 4.7: Total displacement in microgripper 53
Figure 4.8: Stress profile showing maximum stress at a notch hinge 54
Figure 4.9: Voltage vs displacement at jaw graph from FEM 55
Figure 4.10: Voltage vs maximum temperature graph from FEM 55
Figure 4.11: Voltage vs change in average temperature graph from FEM 56
Figure 4.12: Power vs displacement at jaw graph from FEM 57
Figure 5.1: Comparison between displacement from FEM and mathematical model at the jaw 58
Figure 5.2: Comparison between change in average temperature from FEM and mathematical model at the jaw 59

List of Tables

Table 1-1: Comparison of material properties between SU-8 and Silicon [30], [43] 13
Table 2-1: Electrothermal Microgrippers with Important Characteristics 23
Table 3-1: Material Properties [30], [84] 32
Table 3-2: Dimensions of various Parameters with Annotations 33
Table 5-1: Comparison between previous work and this work 61

CHAPTER 1: INTRODUCTION

Technological development today is due to contribution of years of research work and efforts to improve life and help humankind to make this world a better place. With the development of new and reliable research tools makes research work faster and easier. Through time, it has been the primary goal to improve, help and cure the living beings, which involves the study of the cell, a basic unit of life.

This chapter presents an introduction to process and techniques for micromanipulation using various devices. Keeping in view the importance and need of bio manipulation is motivation lying behind the thesis. A brief introduction to the micro-gripper and its application in the field of bio manipulation is presented. Microgripper actuation methods and fabrication techniques are discussed.

1.1 Microgripper Applications

With the advancement in MEMS technology, manipulation of micro objects is becoming a common and essential task. Gripping moving objects with dimensions in microns, taking biological cell and tissue samples is becoming a common task. Previously, micropipetes were used to take biological samples in bulk [1]. Optical tweezers were also used for isolating particles and objects with dimensions in microns. However, it is a difficult and tedious process, and forces are very low [2]. Acoustic traps and magnetic tweezers are some of the other methods. To ease this process, grippers were miniaturized and micro-grippers were introduced.

1.2 Microgrippers

Microgripper is a MEMS device, commonly named as microtweezer, micrograsper and micromanipulator. It is a device that can grip, hold, relocate, rotate, pick and place objects with dimensions in microns. Objects include from components of microrobots to a living cell of various shape and size. This wide range in size of living and non-living objects under observation, leads to variety of microgrippers available today.

Microgripper design varies and improve with advancement in MEMS technology. Variations in a microgripper design are generally based on their actuation method, mechanism, fabrication process and performance. It has wide range of applications depending on above-mentioned characteristics.

Compatibility of a microgripper defines whether it is compatible with certain manipulation task or not. A microgripper should neither physically damage nor chemically react with the object and its surrounding medium. Mechanisms define what kind of motion is required at gripper jaws. High displacement [3], high force [4], parallel motion [5], radial motion [6], dual axis motion [7] etc., are certain types of motion expected at jaws of a microgripper depending on its application. Fabrication process outlines the physical and dimensional limitations and materials used in a design. For various applications, selection materials are considered. For selected materials, different fabrication processes are used. Each process has its benefits as well as limitations.

Comparison can be done between different microgrippers based on their performance. A microgripper is considered better performing if it has lower input electrical power consumption resulting in output higher displacement and higher force at end effector. However, depending on its application, a microgripper should have enough displacement at jaws to grip range of objects it is designed for. On the other hand, jaws of microgripper should be able to provide suitable range of force. Force should be strong enough to grip the object without losing grip and low enough to manipulate the object without damaging it.

1.3 Microgripper Actuation Methods

In MEMS, numerous actuation techniques are available to actuate a microgripper. An actuator takes electrical power as input and results in displacement with some force. Performance of a microgripper highly depends on the performance of an actuator. The better the actuator is, the better the microgripper design is. Ideally, the desirable features of an actuator are low power consumption, small size, large displacement and large force. An actuator must not interact with the object under manipulation process. Most commonly used actuators in a microgripper are electrostatic actuators [8], electrothermal actuators [9] and piezoelectric actuators [10]. Some other types of actuators that can be utilized for microgrippers are shape memory alloy (SMA) actuators

[11], Ionic Polymer Metal Composite (IPMC) actuators [12], hydraulic and pneumatic actuators [13], [14] and electromagnetic actuators [15].

1.3.1 Electrostatic Actuators

Most of first generation microgrippers where actuated using electrostatic actuators. An electrostatic actuator works due to electrostatic forces between two charged beams or plates. Electrostatic forces of attraction are generated. If a set of beams or plates facing each other have opposite charges. For same set of beams or plates, if charges are same, then electrostatic forces of repulsion are produced. If, during actuation, forces of attraction increases and distance between two plates decreases to a certain limit, a phenomenon called pull-in occurs. The voltage at which it occurs is called pull-in voltage. During this phenomenon, oppositely charged plates collide with one another, often damaging the actuator.

Generally, electrostatic actuator are used in the form of large groups to increase its efficiency, which brings us to the downside of electrostatic. This results in large size of an electrostatic actuator, thus increasing the overall size of a microgripper. However, they are easy to control in a certain range. There are three types of electrostatic actuators, parallel plate actuators [16], transverse comb drive [17] and lateral comb drive [18].

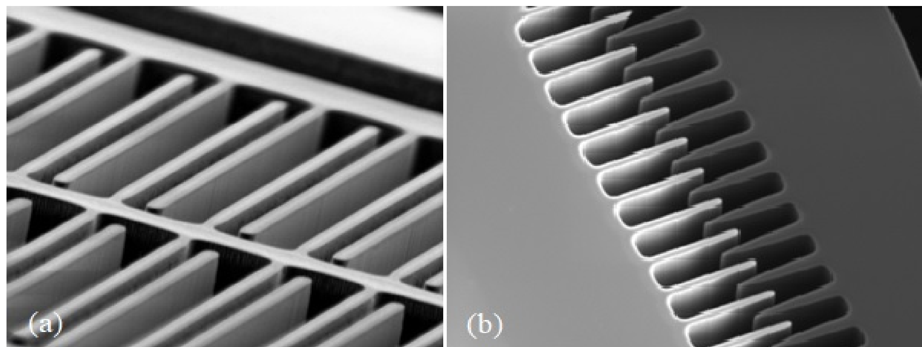

Figure 1.1: Electrostatic actuator types (a) Transverse Comb Drive Actuator [17], (b) Lateral Comb Drive Actuator [18]

Most commonly used type of actuators are lateral comb drives due to their large force but small displacement. Another hardship to overcome in electrostatic comb drives is their small output displacement, which is needed to be amplified, thus, further increasing the overall size of a microgripper. Microgrippers actuated with electrostatic actuators often have electrostatic sensors

for displacement and force sensing which is, sometimes, needed during micromanipulation process to avoid damaging the object. In an electrostatically actuated microgripper, due to electrical charge in the microgripper body, usually during bio-manipulation, it cause the object to stick with microgripper jaws. This requires a separate release mechanism to release the object, hence, further increasing the size of a microgripper.

Unlike electrothermal actuators, there are no high temperatures involved in electrostatic actuators, which is another issue in designing a multipurpose electrothermally actuated microgripper. Electrostatic actuators, require high voltage for actuation, making it impossible to use in fluidic mediums, as it cause the process of electrolysis. Hence, electrostatic actuator based microgrippers are not recommended for biomedical applications.

1.3.2 Piezoelectric Actuators

Piezoelectric actuators uses principle of piezoelectric effect on applying voltage to a piezoelectric material. Applying voltage to opposite surfaces of a piezoelectric material produces strain in material. Depending on the polarity of voltage, strain can be in both directions. If this phenomenon is reversed by applying force to piezoelectric crystal, which results in generation of voltage at opposite surfaces. Due to this behavior, piezoelectric actuator can also act as a sensor. This makes it usable for applications where actuating and sensing is required at the same time, especially in MEMS gyroscope [19] and accelerometer [20]. Piezoelectric materials are also used in actuating and sensing of microgripper [10], [21].

Piezoelectric actuator produces very small displacement and huge force. To increase displacement, piezoelectric crystals are stacked over one another. This increases the size of an actuator. These actuators can operate at high frequency and by reversing polarity, actuators can restore quicker than their elastic restoring forces. Power consumption of piezoelectric actuator is very low and they have long life span.

Piezoelectric actuators have been used with large rigid body multiple displacement amplification mechanisms in microgripper application. These amplification mechanisms increase the overall size of microgripper [10]. High frequency response and high force at the jaws of microgripper can damage the object under manipulation especially in case of biomanipulation. Furthermore, the fabrication process of piezoelectric materials are expensive and output fluctuates

as it follows hysteresis loop [7]. Using piezoelectric actuators in microgripper, with unpredictable motion of microgripper jaws, can result in damage of both gripper jaw and the object.

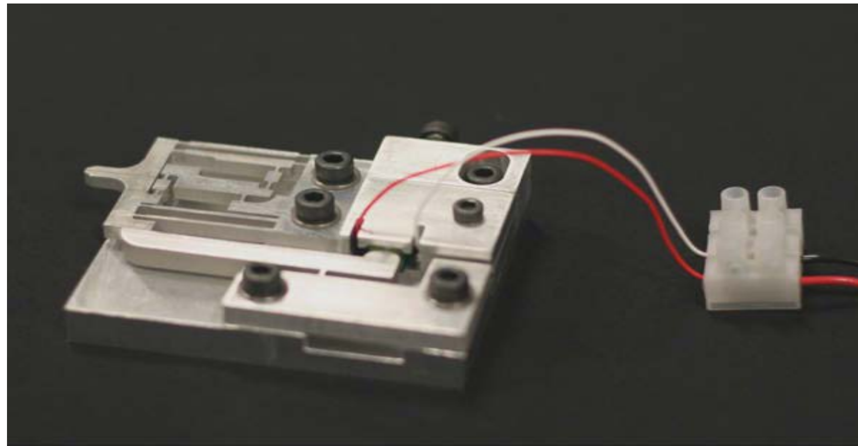

Figure 1.2: Microgripper with piezoelectric actuator and leverage mechanism [7]

1.3.3 Electrothermal Actuators

Electrothermal actuator is an actuator that converts electrical power input in to mechanical output. Now a day, electrothermal actuator is one of the most commonly used actuator in MEMS world. It works on the principle of joule heating and thermal expansion of the material. When a thin electrical wire is connected to an electrical power source, it heats up due to passage of current through it at a certain voltage. With the increases in voltage, the temperature. This electrical wire is attached to a material with coefficient of thermal expansion and desired shape and size, the material expands with the increase in temperature. Thermal expansion in length of a beam is employed to provide force and displacement to a MEMS device such as a microgripper.

While implementing electrothermal actuators, higher the coefficient of thermal expansion of a material, better the performance of an actuator. Electrothermal actuators are compact in size, which make them more feasible for use in MEMS devices. Moreover, power consumption is low. Low actuation voltages of electrothermal thermal actuators make it possible to actuate in an aqueous mediums without. Voltage above 1.229 V can cause electrolysis in aqueous mediums. However, performance of an electrothermal actuator decreases in aqueous mediums due to heat loss. Therefore, power consumption increases while actuating in such mediums.

It is important to make sure that the high temperature from the actuator must not affect its application, an application such as microgripper. Careful design and implementation of electrothermal actuators can easily overcome this obstacle in a MEMS device.

Electrothermal actuators have three basic types. Bimorph electrothermal actuators [22], U-shaped or Guckel electrothermal actuators [27] and Chevron or V-shaped electrothermal actuators [24]. Electrothermal actuators can also be used in groups to increase either displacement [25] or force [26].

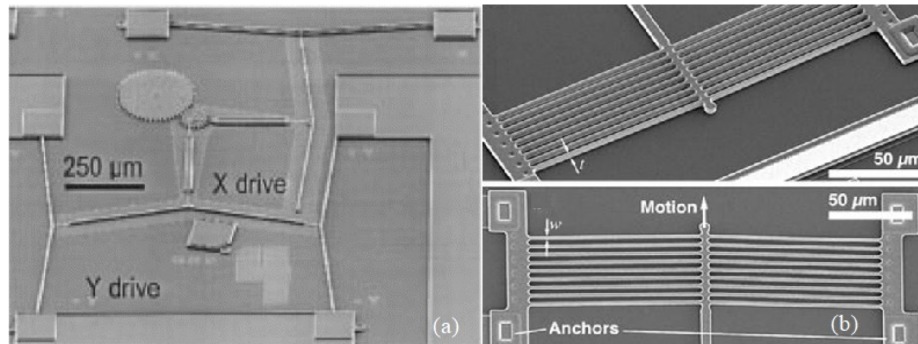

Figure 1.3: Electrothermal Chevron actuator configurations (a) series configuration [25], (b) parallel configuration [24]

Bimorph Electrothermal actuator works like a simple thermostat. However, instead of completing and breaking circuit, it has complete circuit path in it acting as a heater. It consist of two layer to materials, one over another, both with different coefficient of thermal expansion. Upon joule heating, the actuator bends towards the material with low coefficient of thermal expansion. This kind of actuator have undesired two dimensional out of plane motion, usually required to lift something of the plane. A claw like structure with three or more actuators in a circle are used to hold or grip micro objects [27]. Bimorph actuators are rarely used in microgripper application.

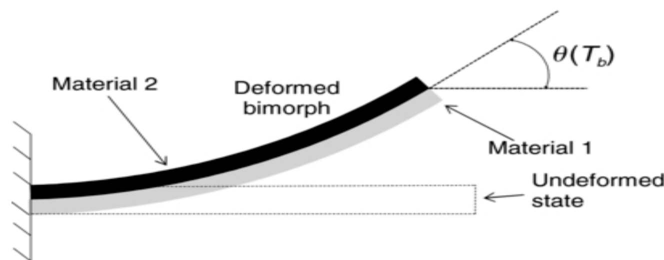

Figure 1.4: Bimorph electrothermal actuator [22]

U-shaped electrothermal actuators usually consist of a hot and cold arm. Electric wire acting as heater is running in U-shape from hot to cold arm. However, there are some versions with U-shaped wire running only through hot arm [28]. The idea is, upon heating of hot arm, the actuator bends towards to the cold arm. Microgrippers using this type of actuator usually show undesired two dimensional motion at jaws making it difficult to grip the object. This two-dimensional motion makes it challenging to use an amplification mechanism with U-shaped electrothermal actuators. Unlike bimorph actuators, U-shaped electrothermal actuators provide in-plane motion.

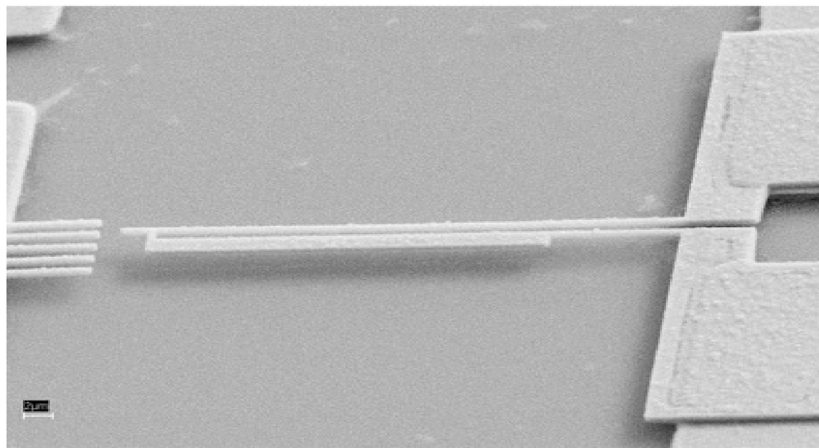

Figure 1.5: U-shaped electrothermal Actuator [23]

Chevron electrothermal actuators are often called V-shaped electrothermal actuators because of their shape looks like alphabet V. Although, the angle between two beams is usually big enough that it might look like a straight line. This type of actuator is well known for its unidirectional output motion. The angle may vary from design to design to get optimized output from actuator. Heater wire is runs from one end to actuator to the other end. Upon joule heating, length of both legs of actuator increases, resulting in common end called shuttle of actuator moving in outward direction [29]. Since both legs are equal in length, hence, equal increase in length under joule heating occurs in opposite direction, the outward motion occurs is unidirectional. This unidirectional motion of chevron actuator can easily be utilized by various displacement and force amplification mechanisms, making it more practical for variety of applications.

The output force and displacement can be increased by adding more chevron actuators, as desired. Adding more chevron actuator in parallel can increase the force of the actuator [26]. On

the contrary, by adding more chevron actuator in series will increase the displacement at the end effector of the actuator [25]. This is the advantage of using chevron actuator over electrothermal actuators. While designing a microgripper, we can benefit from both, actuator output amplification and amplification mechanisms, to achieve huge displacement or force at the jaws, which is desirable. For microgrippers used in biomanipulation, it is necessary to keep the temperature low at jaws to avoid any damage

1.3.4 Other Actuators

There are variety of unique actuators available in MEMS. Some of them are used for actuation of a microgripper. SMA is an actuator that actuate upon heating by passing current through it and retains its original state on cooling. SMA has good actuation speed but sometimes need a restoring force to come back to its original state and are quite expensive to fabricate. In addition, SMA do not return to its original state and show hysteresis which makes is difficult to control and implement in microgripper, especially for bio manipulation. However, there are few microgrippers exists using SMA as actuator [31].

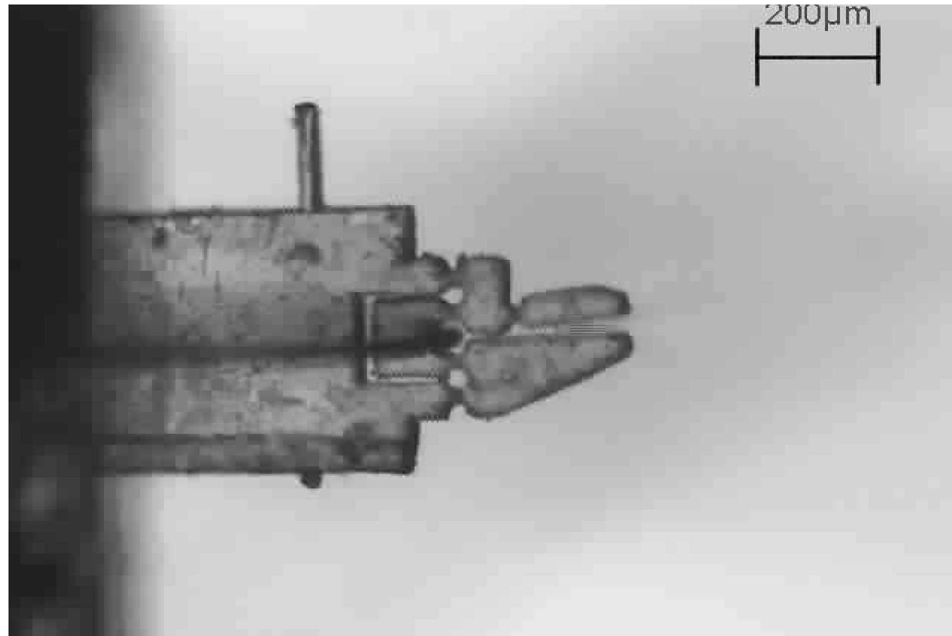

Figure 1.6: Microgripper made of SMA [31]

IPMC is an electroactive material that can be used as an actuator and a sensor in a microgripper [32]. It is a metal sheet cut in various shapes and sizes to develop a microgripper.

Actuation voltage for IPMC is higher than electrothermal actuators. Due to its high voltage, it cannot be used in aqueous medium. Motion at the end effector is not the unidirectional and size of the actuator is big is it requires an assembly to hold actuator in place.

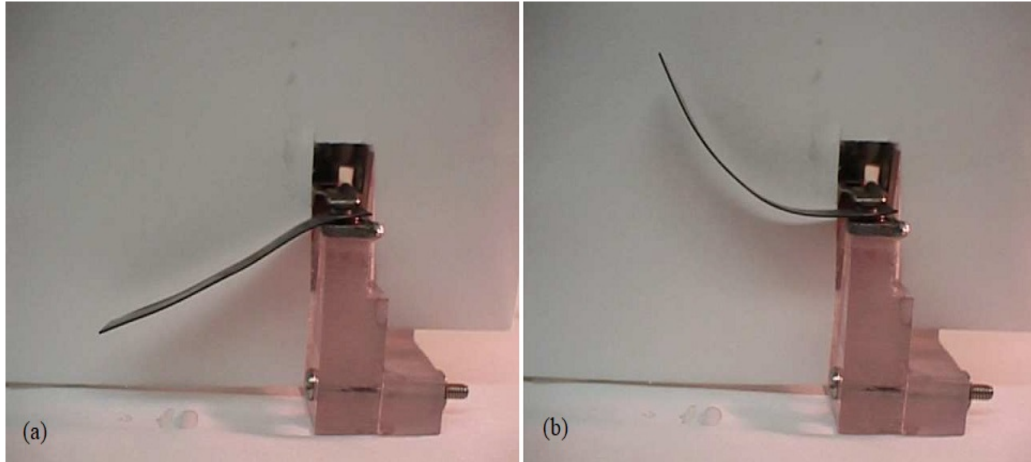

Figure 1.7: IPMC actuator (a) deactivated state, (b) actuated state [32]

Hydraulic [33] and Pneumatic [34] actuators uses pressure from fluids to actuate. Difference between hydraulic actuator and pneumatic actuator is that hydraulic actuator uses liquid to actuate while pneumatic actuator uses air. Both requires a pump with a control system to vary the pressure in actuator and control displacement and force. This increases the size, cost and power consumption of actuator, thus, making them difficult to use in MEMS microgripper. Although, these actuators are bio medically compatible but the cost is too high.

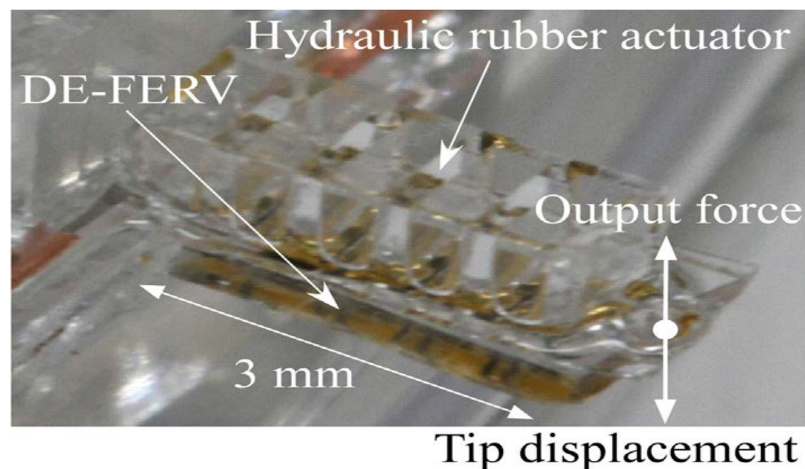

Figure 1.8: Hydraulic Actuator [33]

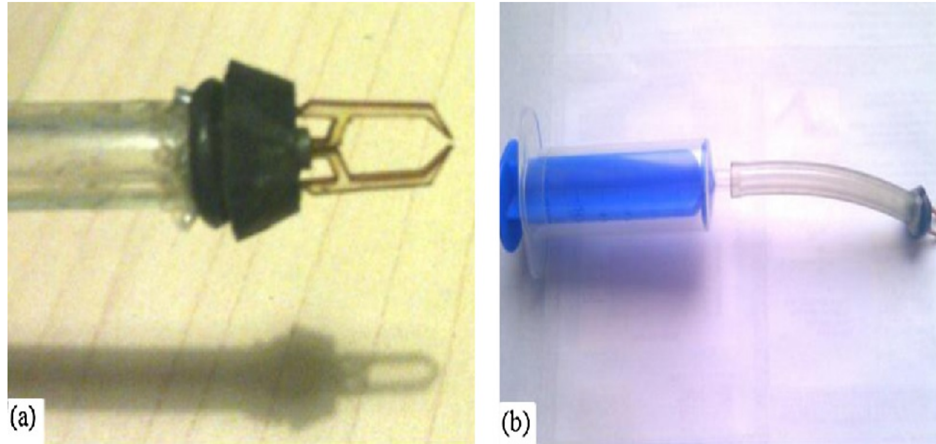

Figure 1.9: Pneumatically actuated microgripper (a) microgripper, (b) actuator [34]

Electromagnetic actuators use magnetic fields to actuate. Voice Coil Motor (VCM) is common type of electromagnetic actuator [35]. VCM implemented in microgrippers, uses electromagnetic field to attract two jaws of microgripper together. Usually, these actuators are made of ferromagnetic materials. In other cases, it uses a pin with linear motion to actuate. However, the size of VCM based actuators are bigger than other MEMS actuators and difficult to scale down. There are untethered micro actuators that only uses magnetic field from various dimensions and angles to move and actuate, used for micromanipulation [36]. This requires huge assembly and, for biomanipulation, magnetic field is not considered healthy.

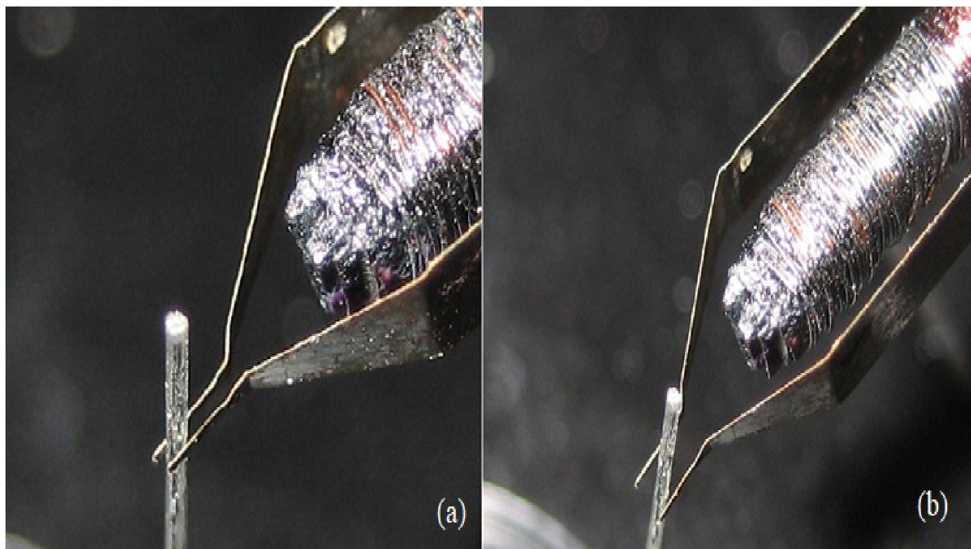

Figure 1.10: VCM based microgripper (a) actuated state, (b) deactivated state [35]

1.4 Microfabrication process

There are various fabrication processes available for fabricating MEMS devices. Processes differ on the basis of material used in fabrication of MEMS device, type of device, feature size and cost. MUMPs stands for multi user MEMS process.

1.4.1 SOIMUMPs

SOIMUMPs stands for Silicon on insulator multi user MEMS process. It is one of the most commonly used process for microfabrication. SOIMUMPs based microgrippers have been fabricated previously with both, electrostatic actuators [37] and electrothermal actuators [38] with high power consumption. Due to high strength and low coefficient of thermal expansion of silicon, very low displacements are achieved at very high temperatures. However, high coefficient of thermal conductivity, those high temperatures reach the jaws of microgripper, making it unusable for biomedical application. Material resistivity can be varied using p-type or n-type doping process.

1.4.2 MetalMUMPs

MetalMUMPs fabrication process uses metal electroplating to fabricate MEMS device. In this process, Nickel is used as a metal for whole device fabrication. A few microgrippers have been fabricated using this process [4]. However, MetalMUMPs is not suitable for fabricating microgrippers with biomedical applications, as of high coefficient of thermal conductivity. High temperature can damage the object under manipulation.

1.4.3 PolyMUMPs

PolyMUMPs stands for polysilicon multi user MEMS process. It is a micromachining process commonly used for fabrication of MEMS sensors. It has three layers, of which, two layers are sacrificial and one metal layer. Seven layers can be formed using up to eight masks. Minimum feature size for this process is 2 μm. Very few microgrippers have been fabricated using this process [40]. Material properties of polysilicon differs for silicon. It has also high coefficient of thermal conductivity, and low coefficient of thermal expansion. Microgripper fabricated from this process have high power consumption.

1.4.4 LIGA process

LIGA is another MEMS fabrication technique, usually used to produce various aspect ratio designs and structures. There are two main types of LIGA fabrication technologies, X-ray based and UV based. X-ray based fabrication is used for high aspect ratio designs while UV based fabrication is for low aspect ratio for designs which is more commonly used. This process consists of three main steps: Lithography, electroplating and molding. This techniques is used to fabricate a few microgrippers [41].

1.4.5 Polymer based fabrication

For past few decades, many MEMS devices have been fabricated using this process. Commonly used polymer is SU-8. SU-8 is an epoxy based negative photoresist. Negative represents, if is exposed to ultraviolet light, the structure become permanent, while unexposed region remain washable. Multiple layers of SU-8 can be added to increase thickness of structure, which also depends on which variant of SU-8 is used. Minimum feature size is 5 µm, however, feature size below 5 µm have also been achieved using complex processes [42]. Polymer based fabricated microgrippers have been fabricated due to SU-8's biomedical compatibility.

1.4.6 Advantages of SU-8

SU-8 polymer has multiple advantages over silicon, polysilicon and metals. SU-8 has many variants, with slight difference in material properties. Besides low coefficient of thermal conductivity of 0.2 W / (m K), it has high coefficient of thermal explosion of 52×10^{-6} 1/m [30]. In addition, it has high electrical resistivity, which aids in isolating electrical circuit from its mechanical end effector. Low coefficient of thermal conductivity do not let high temperatures to reach to jaws of microgripper. For designing better performing electrothermal actuators, high coefficient of thermal expansion is required which SU-8 has. SU-8 based electrothermal actuators have very low electrical power consumption due to very thin metallic heater. Therefore, we choose SU-8 polymer for design of our microgripper.

Table 1-1: Comparison of material properties between SU-8 and Silicon [30], [43]

Material Properties (Units)/Materials	**SU-8**	**Silicon**
Young's Modulus (GPa)	4.60	162
Poison Ratio	0.22	0.22
Density (Kg/m^3)	1200	2320
Specific Heat (J/(kg °C))	1674.8	702
Coefficient of Thermal Conductivity (W/(m °C))	0.2	150
Coefficient of Thermal Expansion (1/ °C)	52×10^{-6}	2.66×10^{-6}

This thesis is organized in following sections. Chapter 2 presents the previously done research on microgrippers with actuators and compliant mechanisms. Chapter 3 describes the proposed designs with mathematical modeling. Chapter 4 verifies the mathematical model by using finite element method tools while chapter 5 explains the results and compare them with detailed discussion. Chapter 6 explains the conclusion and future work.

CHAPTER 2: LITERATURE REVIEW

Like any other research and design process, review of previous work is required. MEMS is an active field of research and a lot of new development done in past few decades. Improvements in modeling and Finite Element Method (FEM) techniques plays an important role in initial design process. With the development of new materials, more efficient fabrication processes, new and improved actuating and sensing techniques, MEMS devices are becoming more efficient day by day. Especially in the field of biomedical instrumentation and sensing.

A review of previously done research work was carried out to design a bio-medically compatible microgripper with better performance and size as small as possible. This literature review of microgrippers is categorized on the basis of actuation principle of a microgripper because it generally defines functionality, applications, cost and mechanisms used in it.

2.1 Electrostatic Microgrippers

Chen et al. [8] reported a design of microgripper with a plunger release mechanism. Both microgripper arms and plunger release mechanism are actuated using electrostatic later comb drives. Microgripper arms can travel only 17 μm closing displacement at 50 V. Overall size of microgripper is $3000 \times 4500 \times 25\ \mu m^3$.

Chen et al. [45], [46] presented a microgripper with four gripper arms to increase gripping range to 100 μm. Arms of this microgrippers are actuated using electrostatic lateral comb drives and gripper arms used piezoresistive sensors for force sensing. In his later work, a microgripper with dual actuators was reported. First one is an electroctatic actuator with lateral comb drives and second one is a pneumatic pump. Large size electrostatic lateral actuators is attached to gripper arm. Both gripper arms have their separate actuators. Total actuation achieved by both arms is 25 μm in fully actuated state at 80 V, the microgripper jaws closes. Since the output displacement of comb drive actuator is very low, length of gripper arms are used as amplification mechanism. The microgripper arms are anchored at a certain point with S-shaped elastic restoring springs to bring jaws back to normal state. This changes to direction of motion and to provide amplified displacement output to grasp object at jaws. After grasping the object, the vacuum pump secures to gripped object. Vacuum pump is used to overcome the van der Waals forces at gripper jaws and

gravitational forces. It can produce negative pressure during pick up and produces positive pressure on release. While releasing of micro balls, it was noticed that, upon release, move to left or right arm, not straight. This was due to adhesion force. This gripper can pick and release object ranging from 100-200 μm.

Khan et al. [47] presented a microgripper design with two different sets of electrostatic actuators for single microgripper arm. The large set of electrostatic lateral comb drive provides driving force and displacement. The second set of electrostatic combs are transverse combs acts as a force sensor and cannot be used as an actuator. The arms of microgripper are anchored to change the direction of motion and provide amplification. Amplification is approximately 4 times the input displacement in this case. Comb drives are attached to cantilever beams, which produce elastic restoring force. To avoid pull-in effect, parasitic capacitance are well covered. 17 μm closing displacement is achieved at 50 V input voltage in this design. This is also a closing microgripper. Total size is $5050 \times 6500 \times 25\ \mu m^3$.

Chang et al. [48] reported a microgripper with rotary comb drives. This design has good output displacement. This microgripper consist of four electrostatic lateral comb drive actuators, two actuators per gripper arm. In this rotary electrostatic actuator, comb drives are different in size. Smaller the radius, shorter the actuator comb. There are 50 comb drives in each actuator, each with different size. Cantilever beams are attached at center of rotary design, which provide restoring force to the microgripper jaws. 94 μm opening displacement is achieved at 100 V in this design. Total size of microgripper is $2900 \times 2700 \times 60\ \mu m^3$.

To measure force at microgripper jaws, Piriyanont et al. [49], [50] presented a design with single actuating arm. Rotary electrostatic four sets lateral actuators are used to actuate the left arm of the microgripper. The right arm of the microgripper is used as force sensing. Rotary differential electrothermal sensors are used due to their compact size. In previous work, author used linear lateral comb drives with linear electrothermal sensor. Although this microgripper is fabricated for biomedical application, temperature at microgripper jaws was not mentioned. Two different type of springs, cantilever beam and S-shaped springs, are used to restore the microgripper to its original state in unactuated from. Length of microgripper arms provide small amplification factor. Electrothermal sensor works on the basic principle of change in resistivity of wire due to change in temperature. Sensor used was DC biased. Sensitivity of force sensor can increase with the

increase in DC voltage of sensor. Sensor input and output showed linear relation. Overall size of microgripper was quite big, $8600 \times 7100 \times 25$ μm^3. 90 μm of opening displacement is achieved on single arm with actuation voltage of 80 V. Sensitivity of 0.55 mV / μN was detected using DC biased voltage of 9.65 V for sensors.

Xu et al. [37] presented another single arm actuated microgripper. The microgripper was single arm actuated with other arm dual axis force sensing. Once again, large set of linear electrostatic lateral comb drive actuator is used to actuate the left arm and linear electrostatic transverse combs were used to sense gripper force as well as environment interaction forces to avoid any accidental damage. Besides cantilever beam springs, multi-stage compound radial flexure (MCRF), rotary bearings, were used to provide elastic restoring force. MCRF in both arms are used to change direction of force and displacement for both actuating arm and sensor. Long microgripper arms provide amplification of 3.11 for the displacement. Size of this microgripper is $4000 \times 5600 \times 50$ μm^3. At actuation voltage of 72 V, actuating arm achieved displacement of 63 μm closing. Force sensor shows sensitivity of 1.45 mV / μN during gripping objects.

Hao et al. [51] reported a microgripper with self-locking ratchet mechanism (ref 9). Both arms of microgripper are actuated using six set of lateral comb drive actuators, three per each gripper arm. Each arm has its own electrostatically actuated ratchet mechanism. Actuating voltage of ratchet is 16 V. 100 μm displacement is achieved at 31.5 V, completely closing gripper jaws.

2.2 Piezoelectric Microgrippers

Chang et al. [52] presented a microgripper actuated using a pair of bimorph piezoelectric actuators. Two bimorph piezoelectric actuators bend toward each other, gripping and object between them. This microgripper is designed to grip wide range of objects, ranging from 0 to 1800 μm in size. There is a linear relationship between input voltage and output displacement. At voltage difference of 200 V, this microgripper can achieve 1200 μm displacement at jaws with initial distance adjustable. Two strain gauge sensor are attached at the base of both cantilever piezoelectric actuators for force sensing. Size of microgripper is $60000 \times 7000 \times 7000$ μm^3.

Xiao et al. [53] reported a piezoelectric microgripper design with parallel motion of jaws and large displacement. Microgripper is actuated using piezoelectric actuator. piezoelectric actuator has large output force and small displacement. So large amplification mechanism is used to achieve displacement of 300 µm is achieved. Mechanism are considered as pseudo rigid body model (PRBM) with flexure hinges. Flexure hinges acts as revolute joint with a torsional spring, which provides elastic restoring force to bring microgripper back to its original position.

Huang et al. [54] presented a microgripper, using piezoelectric actuator, with parasitic motion at jaws using parasitic motion principle (PMP) and PRBM. Links are considered rigid while Circular flexure hinges are considered revolute joints with springs to provide restoring force. With operating voltage range from 25 to 100 V and low frequency of 5 Hz, microgripper achieved parasitic motion at of 20.785 µm at the jaws. Velocity can be varied by increasing and decreasing frequency values. Overall size of the microgripper is in millimeters and whole microgripper is fabricated using electric discharge machining (EDM) from Aluminum alloy.

Sun et al. [55] reported a microgripper with dual amplification mechanism and parallel motion at jaws. Microgripper design is considered a PRBM with first amplification at Scott Russell mechanism and second amplification using Leverage mechanism. Parallelogram mechanism provided parallel motion at jaws of the microgripper. Circular flexure hinges are considered as revolute joints with torsional springs, similar to previous mechanisms. Total displacement of 134 µm after amplification of 15.5 times and actuation voltage for 100 V. This microgripper provides high force at jaws even after large displacement amplification. Overall size of this microgripper is in millimeters using EDM from Aluminum alloy.

Chen et al. [56] presented a microgripper with two degree of freedom (DOF) at jaws. Microgripper is actuated using two separate piezoelectric actuators, one for translational motion and other for rotation. The whole microgripper is considered as PRBM with circular flexure hinges and flexure springs. The left arm of this microgripper translates in X-axis to grip the object while right arm translates in Y-axis to rotate the objects in between jaws. An eddy current based displacement sensor is used for measure output displacement of right arm and strain gauge measures force at tip of left arm. At maximum voltage of 75 V, left jaw translates 190 µm with 4 N force while right jaws translates 85 µm to produce 36° rotation. Over size is in millimeters and design is fabricated using Aluminum alloy.

Xu et al. [57] presented a modular microgripper design with multiple jaws, varying for 2 to 4, each with two DOF motion. Each jaw can travel in both, X-axis and Y-axis, using two separate piezoelectric actuator. Displacement from actuator is transferred to jaw after parallelogram flexure mechanism amplifies it. Amplification factor of 2.43 in X-axis direction and 2.28 in Y-axis direction were calculated.

Zhang et al. [6] reported a piezoelectric microgripper with dual axis motion of object under manipulation at jaws. Size of this microgripper is also in millimeters and fabricated using Aluminum alloy. Actuated using piezoelectric actuators, there are several mechanism employed to get amplified displacement output. The left arm consist of a parallelogram and leverage mechanisms to produce displacement of 108 μm in X-axis, while right arm uses differential amplification mechanism to produce displacement of 223.4 μm in Y-axis direction. Both arm uses circular flexure hinges and parallel cantilever beam springs. Operating at maximum voltage of 75 V, it can rotate object in between jaws up to 90°.

Liang et al. [58] presented a piezoelectric microgripper with parallel motion at jaws. Considering PRBM, each microgripper arm consists of parallelogram leverage mechanism with homothetic bridge mechanism for amplification and parallel motion of jaws. Circular flexure hinges are used as revolute joints with torsional springs. Total displacement of 194 μm is achieved with high force at operating voltage of 150 V. Fabrication and materials used are same as above-mentioned microgrippers.

2.3 Electrothermal Microgrippers

Chronis et al. [59] reported a microgripper with U-shaped electrothermal actuators. Size of the microgripper is $650 \times 100 \times 20$ μm^3. Electrothermal actuator heaters are made of Gold. Gold heaters are usually coated with very thin layer of Chromium to enhance adhesion of Gold with SU-8. 11 μm of displacement at jaws is achieved at voltage of 400 mV and temperature of 57° C.

Voicu et al. [60] presented two microgripper models with a difference of heater position in between SU-8 layers. Outer hot arms are placed at 45° angle, pushing the gripper jaws towards each other. The displacement achieved is 9 μm and 15 μm at maximum temperature of 880° C and

730° C respectively. The maximum voltage used for both microgrippers 0.25 V. size of small microgripper is 400 × 400 × 20.6 μm^3 while size of large microgripper is 800 × 800 × 20.6 μm^3.

Chen et al. [40] reported a microgripper with dual axis motion at both jaws. Microgripper is made of nickel and polysilicon, and actuate using U-shaped hot and cold arm actuator for opening jaws, which is in-plane motion. Second actuator is simple electrothermal actuator which uses thermal expansion to move the jaws upwards for out of plane motion. Displacement of 83.7 µm is achieved using 0.6 V. Total length of microgripper is 2150 µm.

Duc et al. [61] presented a microgripper with two-dimensional motion at jaws, grip and rotate object, using four similar actuators. Total size of the microgripper is 1010 × 740 × 30.6 µm3 and consist of Silicon, SU-8 and Aluminum heater. This microgripper provides 17 µm and 11 µm displacement in X-axis and Y-axis respectively. Power consumption is 35 mW at 2.5 V. Temperature is achieved in this microgripper is just above 200° C and capable to apply forces in micro newtons.

Another design reported by Duc et al. [21] using similar actuator as in above-mentioned design. The microgripper actuators work similar to U-shaped thermal actuator with slight difference of wide arm acting as hot arm and consists of piezoresistive silicon based piezoresistve force sensors. Size of the microgripper is 490 × 334 × 30.6 µm3. Displacement achieved in this design is 32 µm at 180° C and power consumption is 110 mW at 4.5 V.

Colinjivadi et al. [41] presented a SU-8 microgripper for cell manipulation in air and aqueous medium using chevron electrothermal actuator. 25 µm displacement is achieved at jaws using 7.5 mW power consumption, which significantly increases in aqueous medium. Heater is made of thin Gold layer and placed at bottom of chevron actuator.

Solano et al. [28], [62] presented a microgripper for cell manipulation with U-shaped electrothermal actuator. Size of microgripper is 3600 × 520 × 100 µm3 and microgripper is made from SU-8 with Gold heater. In U-shaped actuator, the Gold heater only lies in hot arm while there is no circuit in cold arm. Heater is embedded between two SU-8 layers of different thickness. Total displacement achieved is 110 µm around 1.5 V. Performance of microgripper significantly drops in aqueous mediums, which is increase in power consumption and decrease in displacmenet. Later,

performance of this microgripper is tested in presence of different gases at various pressures. Further, Dodd et al. [63] tested performance of this microgripper at various thickness of SU-8 layer.

Mackay et al. [64], [65] reported an electrothermal microgripper with a modified chevron type actuator. Size of the microgripper is $2000 \times 2000 \times 50\ \mu m^3$ and temperature is kept low in this design. Maximum displacement achieved is 110 µm at 2.8 W with high stresses. However, this microgripper can achieve displacement up to 200 µm, which further increase power consumption and stresses. Copper heater is used with SU-8 in this microgripper. The design is presented again with a force sensor at the bottom of microgripper, increasing the overall size.

Zhang et al. [66] presented a SU-8 based microgripper with PRBM for amplification. Copper based chevron actuators were used and size of gripping mechanism without actuator is $1740 \times 1670 \times 45\ \mu m^3$. 68.5 µm of displacement is achieved at jaws using 108.5 mW power at voltage of 423.1 mV, keeping temperature as low as room temperature at jaws.

Chu et al. [67] presented a similar microgripper design using PRBM for amplification. Size of microgripper with is 3500 × 2900 × 45 µm3 using SU-8 design and copper heater. 107.5 µm displacement at jaws using 25.61 mW power at 73.6 mV voltage. Several other PRBM mechanism are also discussed. Stiffness matrix and kinematic chain method are used to for calculation of this microgripper.

Voicu et al. [68] presented another microgripper design fabricated using SU-8 with Gold heaters. Hot and cold arms type actuators are used to bend simple cantilever beams acting as gripper arms. This microgripper works at high temperature of 1100° C, which SU-8 cannot sustain, to achieve 35 µm displacement at 400 mV voltage.

Soma et al. [69] presented a microgripper for cell manipulation with compact design and unique heater design, containing two U-shaped heaters joined together. Size of microgripper is 1000 × 180 × 20 µm3. At 650 mV voltage, displacement of 21 µm is achieved at 190° C temperature.

Andersen et al. [38] reported a microgripper for manipulation of carbon nanotubes (CNT). This microgripper is fabricated using Silicon. Chevron actuator is used at 8 mA current to get displacement of 2 μm at the jaws.

Kim et al. [70], [71] presented a Silicon based microgripper with chevron actuator. This microgripper consist of dual force capacitive transverse comb sensor, one for measuring gripping force and other for measuring contact force to avoid any damage. Sensors have force resolution of 19.9 nN for gripping force sensor and 38.5 nN for contact force sensor. 65 μm displacement is achieved at jaws using 6 V. Size of the microgripper is 6500 × 5000 × 50 μm3. A heat sink is used between chevron and gripper arm to avoid temperature reaching jaws.

Huang et al. [72–74] presented multiple Silicon based microgrippers using chevron actuators and compliant mechanisms. Trusses and PRBM mechanism are used to achieved small displacements at voltage of 1 to 3 V.

Hoxhold et al. [75] presented a unique microgripper design for bio-manipulation with parallelogram mechanism for parallel motion of jaws and unique actuator. Size of the microgripper is 20000 × 5000 × 321 μm^3. Jaws of this microgripper are bi-directional, open and close. Jaws can travel 26.1 μm using power of 1.79 W at 40 mA current.

Khazaai et al. [4] reported a microgripper with both U-shaped and V-shaped actuator. Total size of the microgripper is 2100 × 1190 × 20 μm3 and made from Nickel. Displacement achieved is 173 μm with approximate holding force of 5 mN. Power consumption is 850 mW at 1 V with temperature reaching 197° C.

Ali et al. [76] presented a microgripper design with chevron actuator and transverse comb drive sensor. Leverage mechanism is used for amplification. Microgripper design is made from nickel and has a total size of 4580 × 2233 × 20 μm^3. 79 μm displacement is achieved at jaws at 700 mV with maximum temperature of 106.15° C.

Demaghsi et al. [77] presented a microgripper to manipulation of nanoparticles and releasing them by vibrating the microgripper arms. Using chevron actuator, 1 μm displacement is achieved at temperature 100° C, using 90 mV of input voltage.

Pasumarthy et al. [78] reported a microgripper design using polysilicon properties and gold heater. Simple U-shaped, hot and cold arm type electrothermal actuators are used to achieved displacement of 67.6 μm at voltage of 3 V. Size of microgripper is only $820 \times 250 \times 15$ μm^3. Large displacement is due to long microgrippers used for amplification.

Shivshare et al. [79] presented a simple microgripper design with chevron actuator directly pushing microgripper arms through heat sinks. Heat sink are used so that actuator temperature does not reach microgripper jaws. Design is modeled using polysilicon properties. 19.2 μm of displacement is achieved at 1 V voltage.

Yang et al. [80] presented a Silicon based microgripper with thermal force sensing and single stage MCRF with single actuating arm. Right arm acts as differential electrothermal force sensor, sensing gripping force and contact force. MCRF is used to change the direction of force and displacement from Y-axis to X-axis and acting as a linear bearing with a spring. Chevron Z-shaped electrothermal actuator is used. Size of the microgripper is $3220 \times 3770 \times 50$ μm^3. 80 μm of displacement is achieved at voltage of 6 V.

Margarita et al. [81] presented a microgripper design with large chevron actuator and U-shaped actuators for locking mechanism. Flexure springs are used to rotate gripper jaws. At voltage level of 5 V, 80 μm displacement with 20mN of force and temperature of 100° C is achieved in this design. Overall size of this microgripper is $600 \times 500 \times 20$ μm^3.

Table 2.1 shows the comparison between some of the electrothermal microgrippers with characteristics discussed in literature review.

Table 2-1: Electrothermal Microgrippers with Important Characteristics

Sr.	Author	Actuation Methods (Electrothermal)	Dimensions: Length × Width × Thickness (μm^3)	Input (Power, Voltage, Current)	Output Displacement (μm)	Temperature (K)	Reference
1	Chronis et al. 2005	U-shaped	650 × 100 × 20	0.400 V	11	330	[59]
2	Voicu et al. 2009	U-shaped	800 × 800 × 20.6	0.250 V	15	1003	[60]
3	Chen et al. 2009	U-shaped + Beam	2150 × - × -	0.600 V	83.7	-	[40]
4	Voicu et al. 2009	U-shaped	400 × 400 × 20.6	0.250 V	9	1153	[39]
5	Duc et al. 2008	U-shaped	1010 × 740 × 30.6	35 mW @ 2.5 V	17	473	[61]
6	Duc et al.2008	U-shaped	490 × 334 × 30.6	110 mW @ 4.5 V	32	453	[21]
7	Colinjivadi et al. 2008	V-shaped	-	0.0075 V	25	-	[41]
8	Solano et al. 2008	U-shaped	3600 × 520 × 100	1.5 V	110	-	[28]
9	Mackay et al. 2013	V-shaped	2000 × 2000 × 50	2.8 W	110	-	[65]
10	Zhang et al. 2011	V-shaped	1740 × 1670 × 45	108.5 mW @ 0.4231 V	68.5	-	[66]
11	Chu et al. 2011	V-shaped	3500 × 2900 × 45	25.61 mW @ 0.0736 V	107.5	-	[67]
12	Voicu et al. 2013	U-shaped	-	0.450 V	35	1373	[68]
13	Soma et al. 2017	Modified U-shaped	1000 × 180 × 20	0.650 V	21	463	[69]
14	Andersen et al. 2008	V-shaped	-	8 mA	2	-	[38]
15	Kim et al. 2009	V-shaped	6500 × 5000 × 50	6 V	65	-	[71]
16	Hoxhold et al. 2010	U-shaped	20000 × 5000 × 321	1.78 W @ 40 mA	26.1	-	[75]
17	Khazaai et al. 2011	V-shaped + U-shaped	2100 × 1190 × 20	850 mW @ 1 V	173	470	[4]
18	Ali et al. 2011	V-shaped	4580 × 2233 × 20	0.700 V	79	379.5	[76]
19	Demaghsi et al. 2014	V-shaped	-	0.090 V	1	373	[77]
20	Pasumarthy et al. 2015	U-shaped	820 × 250 × 15	3 V	67.6	-	[78]
21	Shivhare et al. 2015	V-shaped	-	1 V	19.2	-	[79]
22	Yang et al. 2016	V-shaped	3220 × 3770 × 50	6 V	80	-	[80]
23	Margarita et al. 2016	V-shaped	600 × 500 × 20	5 V	80	373	[81]

CHAPTER 3: PROPOSED MICROGRIPPER DESIGN

Designing micro machines, using MEMS fabrication technique rules, is different from designing large-scale machines. Among various MEMS fabrication techniques, polymer based fabrication technique is selected for designing this microgripper. The polymer commonly used is SU-8. SU-8 is an epoxy based negative photoresist, which has been used for fabricating MEMS device for past few decades.

The reasons for selecting the polymer technique are due to its low cost, biomedical compatibility and low power consumption. Polymer is cheaper than metals and silicon, and easy to use. Biomedical applications require manipulation process at room temperature with no electrical conductivity due to electrolysis. It is compatible with biomedical applications, as it is a non-conductor of electricity and has a very low coefficient of thermal conductivity. Since SU-8 polymer is a non-conductor, thin layers of metals are deposited through electroplating to fabricate electrothermal actuator. Polymer based fabrication is a multi-layer process, so the heater of electrothermal actuator can placed at desired thickness between layers of SU-8. Overall thickness of SU-8 based design can increased by adding more layers of SU-8. Minimum feature size is 5 µm while keeping thickness of the complete structure is 20 µm. To reduce the fabrication cost and complexity, this process requires only two masks for complete fabrication, one for SU-8 structure and one for gold heater and circuit. Proposed microgripper design is shown in figure 3.1 and components are discussed in detail.

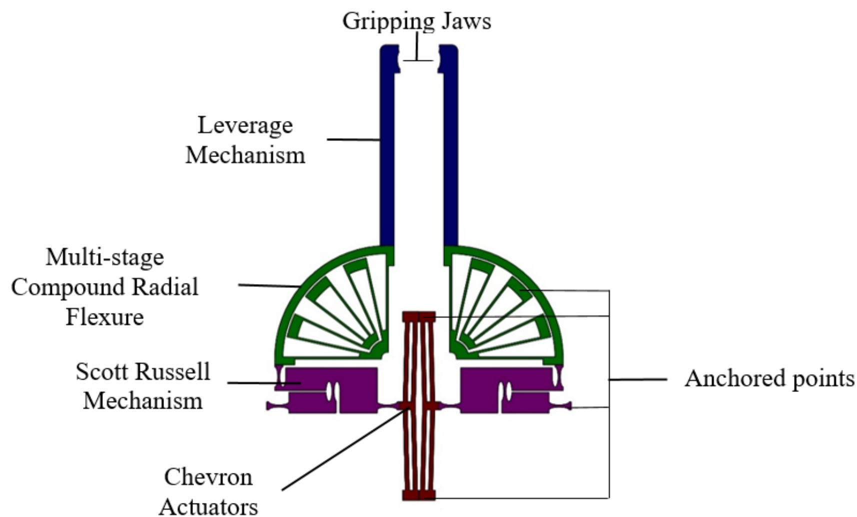

Figure 3.1: Proposed microgripper design with various components mentioned

3.1 Electrothermal Actuator

Among various types of actuators, electrothermal actuators are selected to actuate microgripper arms due to their low power consumption and compact size. Electrothermal actuators work on principles of joule heating and thermal expansion due to increase in temperature. In electrothermal actuators, both bimorph and hot and cold arm actuators do not provide unidirectional motion. On the contrary, chevron actuators provide unidirectional motion with force amplification by adding more actuators. The reason for selecting chevron actuator is most of the compliant mechanism require unidirectional motion as input.

Since the polymer does not conduct electric current, additional layer of metal heater is added to the actuator design. The heater in actuator is made of gold. To avoid any out of plan motion, the gold heater is placed between two layers SU-8 of equal thickness. SU-8 has very poor adhesion with gold. To improve the adhesion of gold with SU-8, very thin layer of chromium is added on top and bottom of gold layer, as chromium has good adhesion with both gold and SU-8. Thickness of gold layer is 300 nm while two layers of chromium have thickness of 10 nm each.

The length of both chevron actuator beams, with its angle, provide displacement at a common point called shuttle and outer ends are anchored. The width of beams and their angle can be optimized to get maximum displacement at minimum power. The width of chevron beams is 10 μm and angle is 1.43°. Two chevron actuators are used in parallel to provide force and displacement for gripping cells of various shapes and sizes. All the important parameters are labeled in figure 3.2 and 3.3.

As the voltage is applied to the opposite and anchored ends of the chevron actuator, temperature of heater increases in the actuator due to joule heating effect. Due to increase in temperature, the length of beams increases and the shuttle moves outwards, providing displacement to the compliant mechanism. However, temperature of heater must not reach above 200 °C, as SU-8 has low melting point. The voltage levels must be kept below 1.29 V, to avoid electrolysis, which is not a problem due to thin heater design.

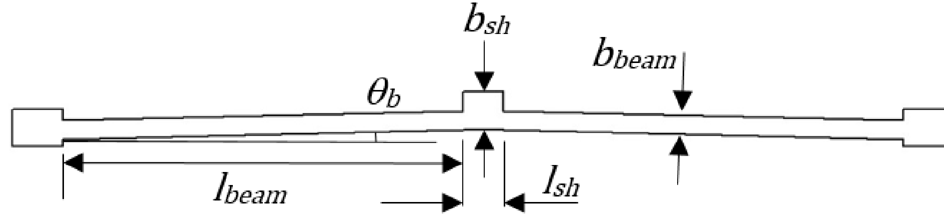

Figure 3.2: Design of actuator with annotations

Figure 3.3: Cross-section of actuator with annotations

3.2 Compliant Mechanisms

3.2.1 Scott Russell Mechanism

Since actuator provides very small displacement, and to increase performance of a microgripper, compliant mechanism are employed. These mechanisms can provide various types of motion. These motions include parallel motion, unidirectional motion, rotational motion, parasitic motion, amplification in displacement or force and changing the direction of displacement and force. To change the direction of displacement from actuator with amplification and place the actuator in such a way that it can be modified, if needed, while reducing the complexity electrical circuit, Scott Russell mechanism provides the solution.

Scott Russell mechanism is a compact mechanism, which provides displacement amplification and change in direction displacement at the same time. It is commonly used mechanism at large scale machines. It consists of two links, one twice the length of second. Small link is fixed at one end and can pivot about fixed end. Other end of small link is attached to the middle of second link and has a pin joint, allowing second link to pivot around it. Now, second link has two free ends, but both are restricted to unidirectional motions at an angle of 90 degrees. One end second link takes input displacement, while other end moves outwards, providing output displacement. Both ends of second link have pin joints and can rotate accordingly. The angle at

which second link is placed, determines how much displacement amplification will this mechanism provide. However, the amplification provided by this mechanism is nonlinear as the angle varies with the input displacement.

In case of MEMS device, Scott Russell mechanism is designed by a different approach. Notches replace all of the pin joints and links are designed as PRBM. Links are considered rigid. Notches are considered revolute joints with torsional springs. Figure 3.4 shows Scott Russell mechanism working principle. Point ‘O’ is the location where small link is fixed and pivots. At point ‘A’, the Scott Russell mechanism takes input in negative X-axis direction. Point ‘B’ is the location where both links are pin joint together through a notch. At point ‘C’, the Scott Russell mechanism provides output displacement, after amplification, through a notch in positive Y-axis direction. Notches are places at points A, B, C and O to replace pin joints at the points and to restore this mechanism to its original state at unactuated state. The length of small link is denoted by ‘l’. The lengths of the links are taken form center of the notches, as the center of a notch acts as a pin joint with a torsional spring.

There are various type of notches are available. Elliptical notches are used to in this design, as they reduce stress concentration at pivoting point and reduce the restoring force on actuator. Dimension variables of important components are mentioned in figure 3.5 below. Scott Russell mechanism has wide range of applications. However, in MEMS, its functionality is limited due to fabrication process constraints. Fabricating parts separately and assembling them increase the cost of fabrication and time. This causes the use of notches as a pin joints.

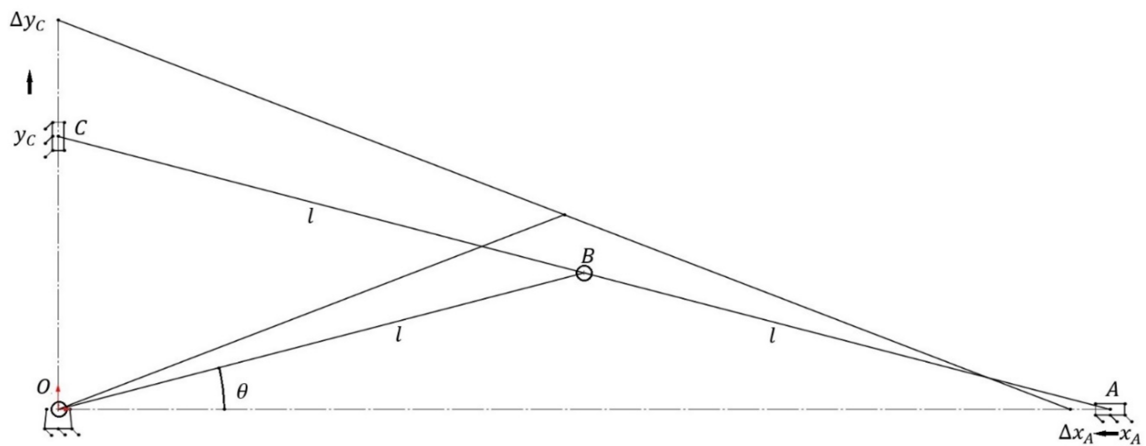

Figure 3.4: Scott Russell mechanism working principle with annotations

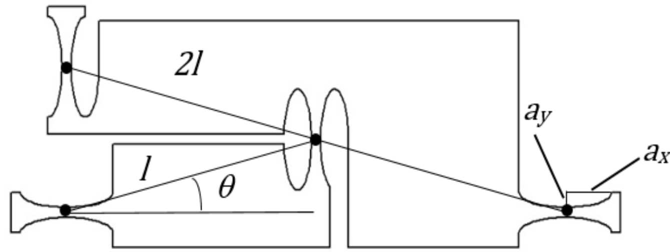

Figure 3.5: Scott Russell mechanism with annotations

3.2.2 Multi-stage Compound Radial Flexure

In past, MEMS devices with radial motion used variety of radial mechanism. In MEMS, making a pin joint for a body to rotate around it is possible. However, it is a tedious and expensive task. In conventional radial flexures, rectangular beams, anchored at pivoting point, are attached radial structure to provide rotational motion. Beams acts as torsional springs upon rotation. Such radial structures provide very limited motion due to high stresses in beams. Conjugate Surfaces Flexure Hinge (CSFH) is another hinge designed to provide radial motion. However, it produces high stresses at large rotations and not suitable for materials like SU-8, which is soft and has a high coefficient of thermal expansion.

To solve this problem, Multi-stage Compound Radial Flexure (MCRF) is used to provide radial motion. MCRF can provide large precise rotations keeping the stresses very low and size compact. It acts as a radial bearing with torsional springs. It has two types and can be modified if required.

MCRF consists of beam like springs acting a torsional springs. The outer and inner radial structures, to which springs are attached, are considered rigid. The inner radial structure is anchored, sometimes at some offset, for pivoting point. Both input and output ends of MCRF have same number of torsional springs, which is the reason for its precise radial motion. It consists of layers of springs that can be modified we desired. The length of all the springs is same for uniform motion. The layers of springs added to MCRF is defined by a variable ‘N’. By increasing the layers of springs, overall length of springs increases while keeping the size same.

The lower end of MCRF is attached to output of Scott Russell mechanism, which is providing input displacement. The upper end of the MCRF is attached to the gripping arm. MCRF does not amplify displacement and input displacement and output displacements are equal. The springs provide restoring force to gripper arm for bring it back to its original state when unactuated. This helps in opening microgripper jaws and releasing objects. Angle between each spring is 12.5 degrees.

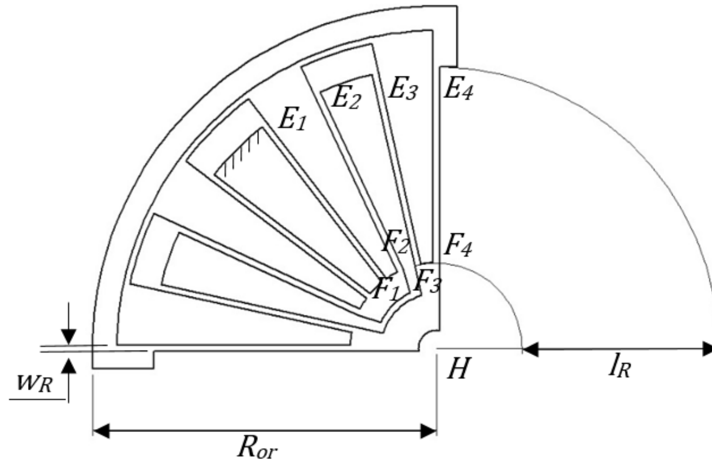

Figure 3.6: Multi-stage Compound Radial Flexure mechanism with annotations

3.2.3 Leverage Mechanism

Leverage mechanism is one the most commonly used mechanism in everyday life. It has been used for centuries to now to move large payloads using small efforts. However, in MEMS, it is used to amplify displacement in most of the scenarios. By taking small input displacement and large force, it amplifies the output displacement and decrease the force by reciprocal of amplification factor. Displacement amplification factor is a ratio, defined as length of moment arm of load from fulcrum to the length of moment arm of effort from fulcrum.

There are three main components in a conventional leverage mechanism, effort, load and fulcrum. Effort is force and displacement applied to the leverage mechanism as input at a certain distance from fulcrum. Load is output force and displacement provided by leverage mechanism to do the required work, also placed at a certain distance from the fulcrum. Fulcrum is a point where the lever is placed, hinged or pin joint, to load it in its position. Leverage mechanism is categorized

in three classes. Position of effort, load and fulcrum on a leverage mechanism defines the class of lever.

Class 1: It is a type of lever with fulcrum in the middle. Load and effort are on the sides.

Class 2: It is a type of lever with load in the middle. Fulcrum lies on one end and effort on other.

Class 3: It is a type of lever with effort is in the middle. Fulcrum and load lies on opposite ends.

In MEMS, fabricating a pin joint is a difficult task from fabrication and assembling point of view, so fulcrum is designed and anchored through flexure springs.in this design, MCRF, a radial bearing, is used to provide the rotation around the pivot. As the effort lies between the fulcrum and the load, this leverage mechanism is classified as class 3 lever. The distance between the MCRF pivoting point to the center of outer beam of MCRF is the moment arm of effort. The distance between the MCRF pivoting point to the tip of gripping arm is the moment arm of load. Figure 3.7 shows the layout of leverage mechanism used in this design.

The length of gripping arm provides amplification in displacement and reduce the undesired motion at jaws in Y-axis direction. The work required to rotate the torsional springs of MCRF and elliptical notches of Scott Russell mechanism, are an additional load on actuator to overcome. This increases the electrical power consumption of chevron actuator, which leads to increase in its temperature. This is the drawback of using flexure springs and notches to avoid complex assembly of pin joints in a microstructure.

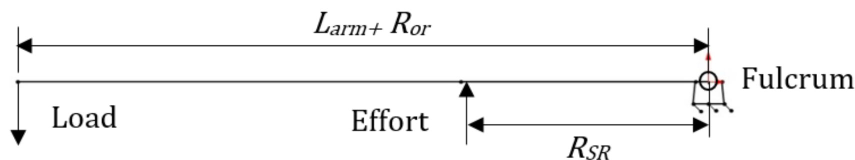

Figure 3.7: Leverage mechanism working principle and annotations

3.3 Gripping Jaws

With the development of microgrippers, various type gripping jaws were mimicked or developed to grip multiple type of objects. Jaws where designed to grip either single type of object

or the objects within a certain range. For biomedical application, design of gripping jaws is a sensitive issue as cells are prone to damage and have multiple limitation. During micromanipulation, micro machine components are very sensitive and, if not properly designed, microgripper can either lose grip of the object or squeeze the object between its jaws. During bio manipulation, cells and tissues are also prone to damage by high temperature and high voltage.

While implementing the electrothermal actuators and compliant mechanisms, these issues where thought through and solved. Use of SU-8 material eliminates the possibility of electrocuting the cells and due to its low thermal conductivity, temperature does not reach the gripping jaws due to chain of compliant mechanisms. Large amplification of both Scott Russell mechanism combine to reduce the force at jaws making it more compatible for bio manipulation.

In past, various gripping jaws where fabricated, including gear teeth jaws, flat face jaws, single and multiple circular jaws and V-cut jaws. All type of jaws have their unique application in the field of micromanipulation. The gear teeth gripper jaws can grip most of the micro object in its range but might damage sensitive objects. Flat faced jaws can grip objects without damaging them but might lose grip and drop the object under manipulation. Circular jaws can only grip round body objects with fixed or larger diameter. V-cut jaws are used to for rotating micro objects under manipulation. For biomedical application and cell manipulation, circular jaws are used.

However, unique gripping jaws are presented in this work. Cells and tissues have various shapes and sizes. To grip the cells of various diameter, a set of dual elliptical jaws are presented. The smaller jaws can grip cells from 3 μm to 10 μm while large set of elliptical jaws can grip cells from 11 μm to 90 μm. The gripper jaws are shown in figure 3.8. The gripping of cells with small diameter range is only possible if the microgripper is fully actuated, closing both jaws. The upper small elliptical jaw has major axis of 5 μm and minor axis of 1 μm, giving to gripping range of 3 μm to 10 μm. The lower large elliptical jaw has major axis of 20 μm and minor axis of 5 μm, hence, giving it the gripping range of 11 μm to 90 μm.

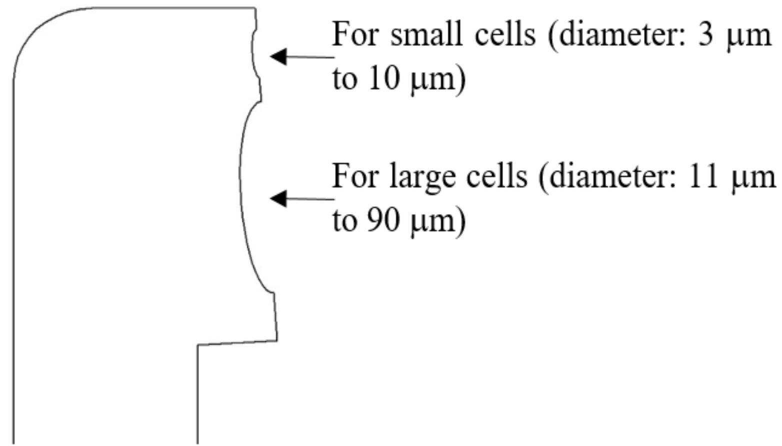

Figure 3.8: Microgripper Jaw

3.4 Mathematical Model of Proposed Microgripper Design

To evaluate the mathematical model of this microgripper, spring constants of in Scott Russell mechanism and MCRF mechanism are needed to be calculated. Material Properties SU-8 and Gold used for mathematical model are given in table 3.1 and all the important dimensions with annotations are mentioned in table 3.2.

Table 3-1: Material Properties [30], [84]

Material Properties	SU-8	Gold	Units
Young's Modulus	4.60	70	GPa
Poison Ratio	0.22	0.35	-
Density	1200	19320	Kg/m^3
Specific Heat	1674.8	128	J/(kg °C)
Coefficient of Thermal Conductivity	0.2	300	W/(m °C)
Coefficient of Thermal Expansion	52×10^{-6}	14.2×10^{-6}	1/ °C
Electrical Resistivity	-	2.4e-8	Ω m

Table 3-2: Dimensions of various Parameters with Annotations

Parameter	Representation	Value	Unit
Thickness of micro structure	h	20	μm
Thickness of notch	t	5	μm
Ellipse major axis ($a_x > a_y$)	a_x	25	μm
Ellipse minor axis	a_y	7.5	μm
Scott Russell mechanism angle	θ	15	°
Width of MCRF springs	w_R	5	μm
Outer radius of MCRF springs	R	230	μm
Inner radius of MCRF springs	r	70	μm
Outer radius of MCRF structure	R_{or}	280	μm
Position where Scott Russell applies input in X-axis	R_{SR}	270	μm
Number of spring stages in MCRF	N	2	-
Length of MCRF springs	l_R	160	μm
Length of microgripper arm	L_{arm}	500	μm
Microgripper arm radius of rotation	L_{rt}	780	μm
Number of chevron actuators per gripper arm	n	2	-
Thickness of SU-8 layer on actuator	$h_{SU\text{-}8}$	20	μm
Thickness of Gold heater layer	h_{Au}	0.32	μm
Vertical length of actuator beam	l_{beam}	200	μm
Angle actuator beam with vertical line	θ_b	1.43	°
Length of actuator beam	l_o	199.93	μm
Width of actuator beam	b_{beam}	10	μm
Length of shuttle	l_{sh}	20	μm
Width of shuttle	b_{sh}	20	μm

To know the amount of work done by actuator due to presence of torsional springs in the system, and to grip an object, if there is any, a basic equation of work is derived. To calculate the power required, we need to calculate the stiffness of torsional springs.

$$F_A x_A = F_{out} x_{out} + k_{SR} {x_A}^2 + k_R \, {\theta_R}^2 \tag{3.1}$$

Using the model provided [44], first stiffness of a single notch is calculated. For an elliptical notch, β_x and β_y are calculated, which depends on the dimensions of notch.

$$\beta_x = \frac{t}{2a_x} \tag{3.2}$$

$$\beta_y = \frac{t}{2a_y} \tag{3.3}$$

From equation (2) and (3)

$$\varepsilon = \frac{a_x}{a_y} = \frac{\beta_y}{\beta_x} \tag{3.4}$$

Where ε determines the ratio of major and minor axis of ellipse. The $f(\beta_x)$ is a function depending on β_x, which estimates the accurate stiffness of a notch.

$$f(\beta_x) = \left[\frac{1}{2\beta_x + {\beta_x}^2}\right] \times \left[\left(\frac{3 + 4\beta_x + 2{\beta_x}^2}{(1+\beta_x)(2\beta_x + {\beta_x}^2)}\right) + \left(\frac{6(1+\beta_x)}{(2\beta_x + {\beta_x}^2)^{\frac{3}{2}}}\right) tan^{-1}\left(\sqrt{\frac{2+\beta_x}{\beta_x}}\right)\right] \tag{3.5}$$

Using the stiffness model of an elliptical notch and replacing the variables, spring constants of notches used in Scott Russell mechanism are calculated as k_i and given by following equation.

$$k_i = \frac{2Eha_x{}^2}{3\varepsilon^3 f(\varepsilon\beta_x)} \tag{3.6}$$

There are four notches in Scott Russell mechanism with same size and dimensions. To calculate the total spring constant of hinges A, B, C and O, equation (3.6) is used [55], and represented by k_{SR} in equation (3.7).

$$\sum_{i=A}^{O} k_i \theta_i = k_A \theta_A + k_B \theta_B + k_C \theta_C + k_O \theta_O$$

Where $i = A, B, C, O$ and converting rotational motion to translational motion by finding angle in terms of actuator input displacement x_A to the mechanism, we get $\theta_A = \frac{x_A}{2l\,sin\,\theta}$, $\theta_B = \frac{x_A}{l\,sin\,\theta}$, $\theta_C = \frac{x_A}{2l\,sin\,\theta} - \frac{x_A\,cot\,\theta}{R_{SR}}$ and $\theta_O = \frac{x_A}{2l\,sin\,\theta}$. Using all angles, we get total stiffness of Scott Russell mechanism.

$$k_{SR} = \frac{k_A}{(2l\sin\theta)^2} + \frac{k_B}{(l\sin\theta)^2} + k_C\left(\frac{1}{2l\sin\theta} - \frac{\cot\theta}{R_{SR}}\right)^2 + \frac{k_O}{(2l\sin\theta)^2} \tag{3.7}$$

To calculate amplification of Scott Russell mechanism [85], l represents the length of small link OB and θ represents the angle of mechanism with X-axis.

$$AB = OB = BC = l \tag{3.8}$$

$$\angle OAC = \theta \tag{3.9}$$

Length of link AC is $2l$ and using Pythagoras theorem,

$$x_A{}^2 + y_C{}^2 = 4l^2$$

$$y_C = \sqrt{4l^2 - {x_A}^2}$$

Motion of link end at point C is along Y-axis only, hence,

$$x_c = 0$$

Again using Pythagoras theorem on link AC, we get,

$$(x_A + \Delta x_A)^2 + (y_C + \Delta y_C)^2 = 4l^2$$

$${x_A}^2 + {y_C}^2 = (x_A + \Delta x_A)^2 + (y_C + \Delta y_C)^2$$

$$(y_C + \Delta y_C)^2 = {x_A}^2 + {y_C}^2 - (x_A + \Delta x_A)^2$$

$$y_C + \Delta y_C = \sqrt{{x_A}^2 + {y_C}^2 - (x_A + \Delta x_A)^2}$$

$$\Delta y_C = -y_C + \sqrt{{y_C}^2 - 2x_A \Delta x_A - {\Delta x_A}^2}$$

Which indicates a nonlinear relationship between Δy_C and Δx_A. As Δx_A approaches zero, i.e., $\Delta x_A \rightarrow 0$, the relation can be expressed in the form:

$$Amp_{SR} = \frac{\Delta y_C}{\Delta x_A} \approx \frac{dy_C}{dx_A} = -\frac{x_A}{\sqrt{4l^2 - {x_A}^2}} = -\frac{x_A}{y_C} = -\cot\theta \tag{3.10}$$

Where Amp_{SR} is the amplification and depends on θ. Amplification is only possible if θ has range of $0 < \theta < \pi/4$.

The displacement from Scott Russell mechanism enters MCRF after amplification. The MCRF has torsional springs and to calculate the spring constant, model is given [86]. Since the motion of the MCRF is radial and it rotates by angle θ_R, as mentioned above in total work equation, $\theta_R = y_C / R_{SR}$ which gives displacement. The k_R represents the total stiffness of MCRF and given as following.

To calculate the rotary angle of the primary stage, the deformations of the four flexures E_iF_i, where $i = 1,2,3,4$ are shown in figure 3.6. A flexure under goes moment m as well as a force f along the tangential direction. Due to force and moment, flexure travels the displacement d along the tangential direction. This translation of the free end F_1 is considered rotating around pivoting point H by an angle θ_1. Using these conditions, following relations are derived:

$$0 = \frac{f{l_R}^2}{2EI_R} - \frac{ml_R}{EI_R} \tag{3.11}$$

$$d = \frac{f{l_R}^3}{3EI_R} - \frac{m{l_R}^2}{2EI_R} \tag{3.12}$$

Where E is the Young's modulus of SU-8 and $I_R = hw_R^3/12$ is the area moment of inertia of the spring. The moment m can be solved from Eq. (3.11) as follows:

$$m = \frac{fl_R}{2} \tag{3.13}$$

As the rotation in each spring is small, the angle θ_1 is considered as displacement d as follows:

$$\theta_1 = \frac{d}{r} \tag{3.14}$$

The flexure E_2F_2 is rotated at angle θ_1 due to the deflection of E_1F_1. Since the E_2F_2 is same as E_1F_1, the free end E_2 also translates by d. Hence, the angle of rotation of flexure E_2F_2 about point H can be given as follows:

$$\theta_2 = \theta_1 + \frac{d}{R} \tag{3.15}$$

Similarly, angle for flexures E_3F_3 and E_4F_4 are calculated as follows:

$$\theta_3 = \theta_2 + \frac{d}{r} \tag{3.16}$$

$$\theta_4 = \theta_3 + \frac{d}{R} \tag{3.17}$$

Substituting equations (3.14), (3.15) and (3.16) into Eq. (3.17) gives,

$$\theta_4 = 2d\left(\frac{1}{R} + \frac{1}{r}\right) \tag{3.18}$$

Then, substituting equations (3.12) into Eq. (3.14) after substituting Eq. (3.13) allows the calculation of the rotary angle:

$$\theta_4 = \frac{f{l_R}^3(R + r)}{6EI_R Rr} \tag{3.19}$$

MCRF has two sets of flexures, with two basic modules, i.e., $N = 2$. In general, MCRF can be represented as follows:

$$\theta_R = \frac{Nf{l_R}^3(R + r)}{12EI_R Rr} \tag{3.20}$$

Where N is the number of layers in secondary stage. At equilibrium, sum of the moment about the center point H, the following equation can be derived:

$$2fR - 2m - M = 0 \tag{3.21}$$

Solving for moment M from Eq. (3.11) and using Eq. (3.3) gives

$$M = 2fR - fl_R \tag{3.22}$$

Using the equations (3.12) and (3.10), the torsional spring constant of a general MCRF can be calculated as follows:

$$k_R = \frac{M}{\theta_R} = \frac{12EI_R Rr}{N{l_R}^3} \tag{3.23}$$

The second amplification mechanism in this design is leverage mechanism. Class 3 lever is used to amplify the displacement. The variable Amp_R represents the amplification factor and calculated as:

$$L_{rt} = L_{arm} + R_{or} \tag{3.24}$$

$$Amp_R = \frac{L_{rt}}{R_{SR}} \tag{3.25}$$

To calculate the total stiffness, substitute the values of spring constants in total work equation (1), which gives us,

$$F_A x_A = F_{out} x_{out} + k_{SR} {x_A}^2 + k_R \, {\theta_R}^2$$

$$F_A x_A = F_{out} Amp_{tot} x_A + k_{SR} {x_A}^2 + k_R \left(\frac{y_C}{R_{SR}}\right)^2 \quad (3.26)$$

$$F_A = F_{out} Amp_{tot} + \left(k_{SR} + k_R \frac{Amp_{SR}}{R_{SR}}\right) x_A \quad (3.27)$$

$$F_A = F_{out} Amp_{tot} + k_{eq} x_A \quad (3.28)$$

A Chevron actuator, electrical power as input to produce heat and increase in temperature, and hence thermal expansion providing displacement and force to compliant mechanism. As this a multi domain physics problem, some constraints are set; convection on actuator surfaces and substrate is ignored, actuator arms lose heat through anchor points, thermal expansion of actuator beams are considered and material properties dependent on are considered constant (ref 5). The thermal model of joule heating and change in temperature due to conduction is given by following equation [29], [85].

$$k \frac{d^2 T}{dx^2} + \dot{q}_b + \dot{q}_s = 0 \quad (3.29)$$

Where k is the thermal connectivity of thin film gold heater. In the above equation $k \frac{d^2T}{dx^2}$ describes the heat conduction in the microstructure while $\dot{q}_b$ and $\dot{q}_s$ are the joule heat sources in the actuator beam and shuttle respectively and can be computed as:

$$\dot{q}_b = \frac{{A_{sh_Au}}^2}{\rho_{Au} \left(2 l_{beam} A_{sh_Au} + n l_{sh} A_{beam_Au}\right)^2} V^2 \quad (3.30)$$

$$\dot{q}_s = \frac{\left(n A_{beam_Au}\right)^2}{\rho_{Au} \left(2 l_{beam} A_{sh_Au} + n l_{sh} A_{beam_Au}\right)^2} V^2 \quad (3.31)$$

Where ρ_{Au} is the electric resistivity of gold, n is the number of chevron actuators, $A_{sh_Au} = w_{sh}t_{Au}$ and $A_{beam_Au} = w_{beam}t_{Au}$ are the cross-sectional area of the gold layer in the actuator beam and shuttle respectively. The thermodynamic equation can be solved respecting the boundary conditions that the temperature at anchors is at room temperature T_0 during operation and due to symmetry, the temperature of the micro beams and shuttle at $x = l_{beam}$ and $x = l_{beam} + l_{sh}$ are the same and the rate of heat conduction at $x = l_{beam}$ and $x = l_{beam} + l_{sh}$ are the same. The average change in temperature can be obtained as:

$$\Delta T_{avg} = PQV^2 \tag{3.32}$$

Where $P = \frac{1}{12k_{Au}\rho_{Au}}$ and $Q = \frac{A_{su_Au}l_{beam}(4l_{beam}A_{sh_Au}+3nl_{sh}A_{beam_Au})}{(2l_{beam}A_{sh_Au}+nl_{sh}A_{beam_Au})^2}$. The equation (32) shows that the average change in temperature in the embedded gold layer in the V-shaped actuator beams and shuttle can be determined by the material properties *P*, geometry Q of V-shaped beam and shuttle and input voltage.

By considering the steady-state temperature increase ΔT_{avg} in the gold layer, and assuming that same temperature would be conducted to upper and lower SU-8 layer at steady-state regardless of thermal conductivity of the SU-8 layers, the elongation in the SU-8 beams respectively. ΔL_{Temp} can be obtained as:

$$\Delta L_{Temp} = \alpha_{SU-8}\Delta T_{avg}l_{beam} \tag{3.33}$$

Where α is the coefficient of thermal expansion of SU-8. With linear deformation assumption of the actuator beams, the displacement of shuttle can be estimated using the Castigliano's theorem. The output displacement produced by actuator, which also acts as an input displacement for the Scott Russell mechanism and can be written as:

$$x_A = \alpha_{SU-8}J_1\Delta T_{avg} - \frac{1}{2nE_{SU-8}}J_2F_A \tag{3.34}$$

Where E is the Young's Modulus of SU-8, $J_1 = l_{beam}J\sin\theta_{beam}$, $J_2 = \frac{l_{beam}J}{A_{beam_SU-8}}$ and $J = \frac{{l_0}^2}{{w_{beam}}^2\cos^4\theta_{beam}+{l_0}^2\sin^2\theta_{beam}}$.

By putting the value of ΔT_{avg} from equation (3.32) into equation (3.34) we get,

$$x_A = P_1V^2 - P_2F_A \tag{3.35}$$

Where $P_1 = \alpha_{SU-8}J_1QP$ and $P_2 = \frac{J_2}{2nE_{SU-8}}$. Since $F_A = F_{out}Amp_{tot} - k_{eq}x_A$, equation (35) can be written as:

$$x_A = P_1V^2 - P_2\left(F_{out}Amp_{tot} - k_{eq}x_A\right) \tag{3.36}$$

$$x_A = \left(\frac{P_1V^2 - P_2F_{out}Amp_{tot}}{1 + P_2k_{eq}}\right)Amp_{tot} \tag{3.37}$$

$$x_A = S_1V^2 - S_2F_{out} \tag{3.38}$$

Where, S_1 and S_2 are system's compliance shown to the applied actuation voltage to the actuator and external force applied on the gripping jaws respectively and can be represented as $S_1 = \frac{P_1}{1+P_2k_{eq}}$ and $S_2 = \frac{P_2Amp_{tot}}{1+P_2k_{eq}}$.

$$F_{max} = \frac{S_1}{S_2}V^2 \tag{3.39}$$

The force F_{max} is the maximum output force provided at the gripping jaws.

3.5 Results

Using above mathematical model of the microgripper in Matlab software, results are generated using voltage from 5 mV to 50 mV. To ensure the design is valid and gives desired

performance characteristics and to compare it with other designs, these results are compiled. The characteristics include displacement and force at jaws, temperature and input power consumption.

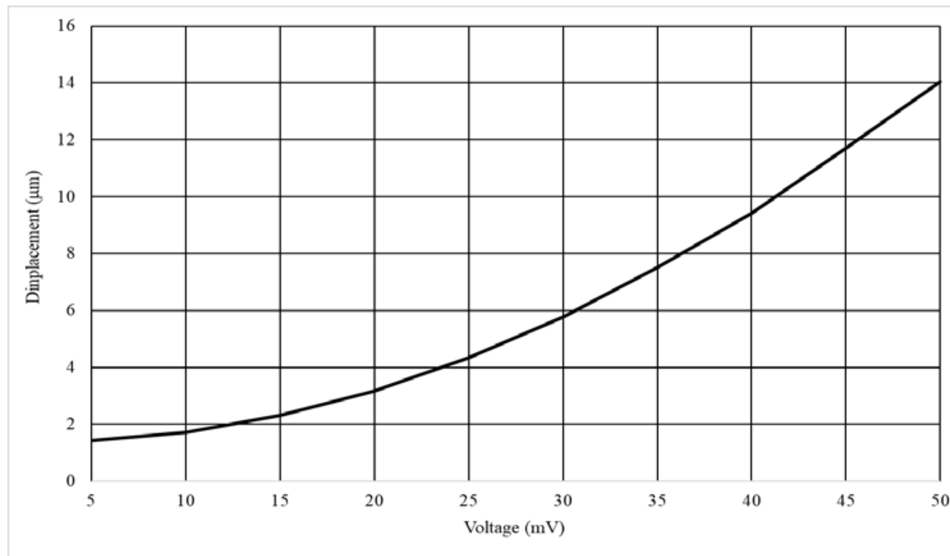

Figure 3.9: Voltage vs displacement graph from mathematical model

Figure 3.9 is a graph between applied input voltage and displacement at the jaws of the microgripper. With the increase in voltage, displacement at the jaws increase. This graph shows a nonlinear response of displacement with respect to the voltage. At voltage of 50 mV, 14 μm displacement is achieved at the jaw without the presence of any force on the jaw.

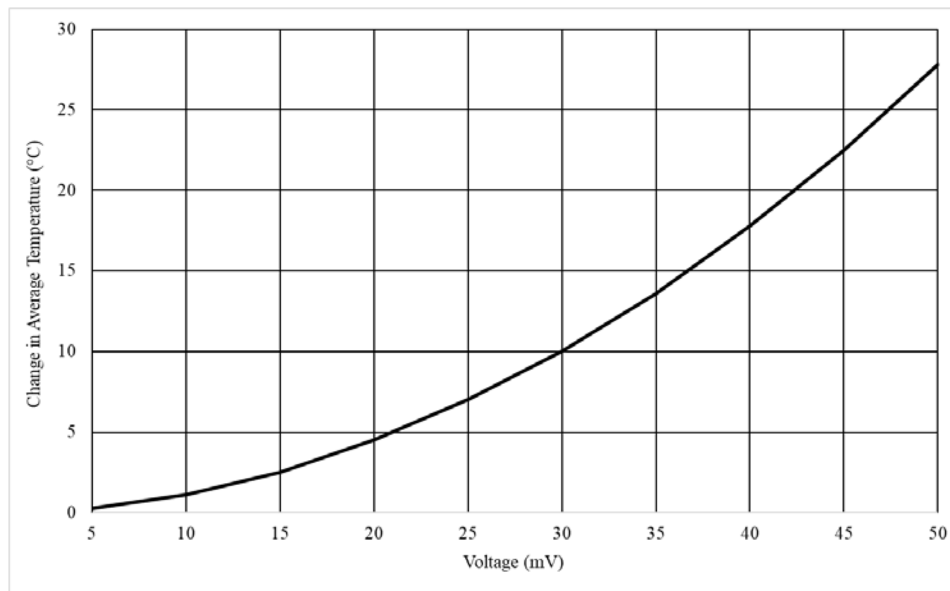

Figure 3.10: Voltage vs average change in temperature graph from mathematical model

Figure 3.10 results of voltage vs change in average temperature are shown. Change in average temperature is the difference of average value of temperature with respect to initial temperature in actuator beams. Response from this graph describes the response of displacement at jaw with respect to the voltage. Since the graph is nonlinear, so is the graph between voltage and displacement at jaw. Nonlinear behavior is due to non-uniform increase in temperature with the increase in voltage. Maximum temperature difference of average temperature and initial temperature is 27.8 °C at 50 mV.

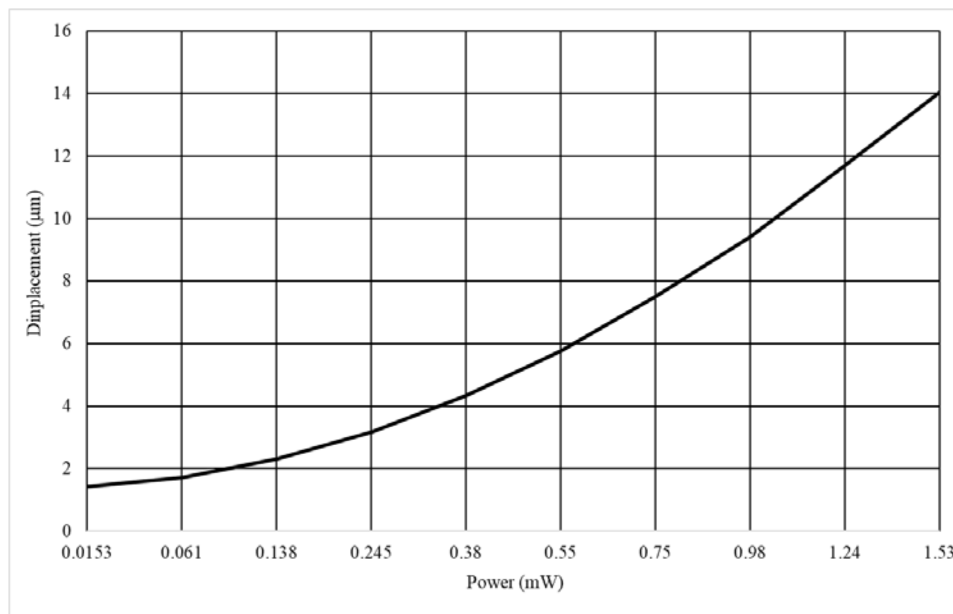

Figure 3.11: Power vs displacement graph from mathematical model

As mentioned above, graph in figure 3.11 between input power and displacement shows the similar nonlinear trend due to nonlinear increase of change in average temperature. Using electrical power formula in terms of input voltage and actuator heater resistance, maximum power consumption of 1.53 mW is evaluated at 50 mV for single gripping arm.

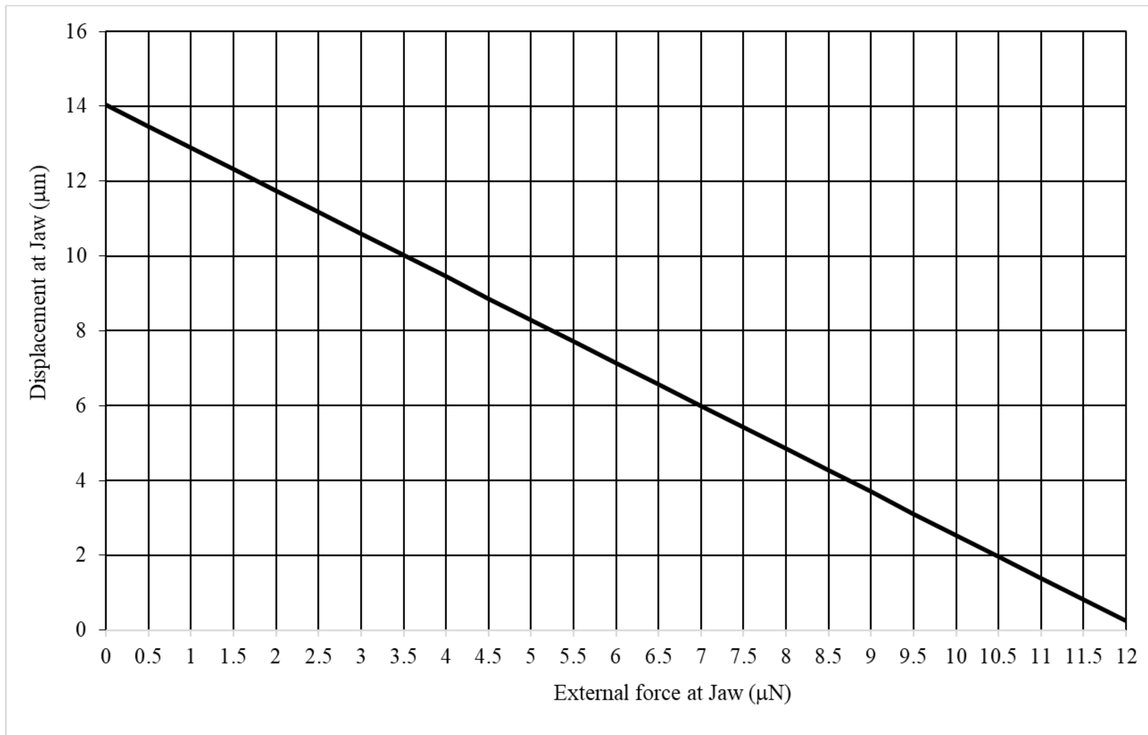

Figure 3.12: External force vs displacement graph from mathematical model

Figure 3.12 shows graph between the external force at jaw and displacement at jaw. External force and displacement at jaw are inversely proportional to each other and shows a linear behavior. With increase in force at the jaw while gripping object, displacement decreases. This graph aids in manipulating sensitive object like cells, which are prone to damage due to high gripping force at the jaw.

CHAPTER 4: VERIFICATION OF MICROGRIPPER DESIGN

4.1 Finite Element Method

To verify the validity of any design, various methods are available. Finite Element Method (FEM) is one the best way to ensure microgripper design is flawless and works accordingly to fulfill its purpose. Mathematical model gives the estimated results and does not show where the problem might occur. However, FEM helps in verifying the results from mathematical model as well as helps us visualize the problems that might occur in the design. From determining solutions to finding problems and design flaws in a design, FEM can do that in multiple and hybrid domains. In MEMS, prototyping and fabrication is expensive and time consuming, varying from process to process. Therefore, validating a design before fabrication through FEM is a good idea.

A design is modeled on a modeling software, SolidWorks. Design files are imported to FEM tool for analysis. Analysis are carried out on a well-reputed FEM tool, Ansys, as it can solve problems from multiple and hybrid domains. Since our design is a multi-domain physics problem, electrical, thermal and structural analysis are done to visualize to design at various stages. Effects of changing loading conditions can be studies using FEM to find the optimal solution for a microgripper. FEM method is computationally expensive and time consuming, hence, for ease, only half of the microgripper is simulated, as both halves are similar and perform the same.

4.2 Initial Loading Conditions

Loading conditions are the initial and constant loads on a system that effects is performance during a simulation. These conditions can be due to the surrounding of a system or location where is placed. Since we are interested in electrical, thermal and structural analysis, multiple loading conditions are involved in different domains.

Initially, material properties are defined for both SU-8 and Gold. All the temperature dependent properties are considered constant due to small change in temperature is expected. Afterwards, design files are imported from SolidWorks after modeling and assembling. Half of the microgripper under simulation has four anchored points with the substrate, which holds the microstructure in its place. microgripper in unactuated state, has no electrical power through the heater wires in it. Hence, there is no initial electrical load. As the device is considered to be placed

in a room with controlled temperature of 25 °C, whole device is considered at room temperature due to conduction through anchored points. Rate of conduction depends on material properties of SU-8 and gold. Convection and radiation has very small effect on MEMS devices. Rate of convection varies with change in surrounding medium. Surrounding medium is considered air with a constant convective heat transfer rate of 20 W/(m^2 °C) at the temperature of 25 °C on the surface of gripping arms and jaws. For structural analysis, all the anchored points are considered rigid with no degree of freedom at all. To simulate the microgripper, two anchor points, the outer ends of actuator are applied with electrical power, which is varied to see response of microgripper at various stages. Material properties are mentioned in table 3.1 in chapter 3.

4.3 Analysis Types

Two types of analysis are carried out for observing responses in three different domains, which includes electrical, thermal and structural. Initially electrical power is applied to the microgripper, resulting in change in temperature and thermal expansion. Thermal expansion causes structural changes and motion of jaws and other parts of the microgripper. Two types of static analysis include Thermal-Electric analysis and Static Structural analysis. Mesh type and size selection improves results. The smaller the mesh element size, the better the results will be. However, smaller mesh size increase the computation cost and simulation become impossible to perform. Ansys automatically select mesh element type, which SOLID90 for SU-8 and SOLID226 for gold for coupled field analysis. General mesh size is kept 5 μm while front face mesh size of whole design is kept 2.5 μm. Mesh size smaller than above mention size causes the simulation to fail. Figure 4.1 shows the meshing diagram of various components of a microgripper.

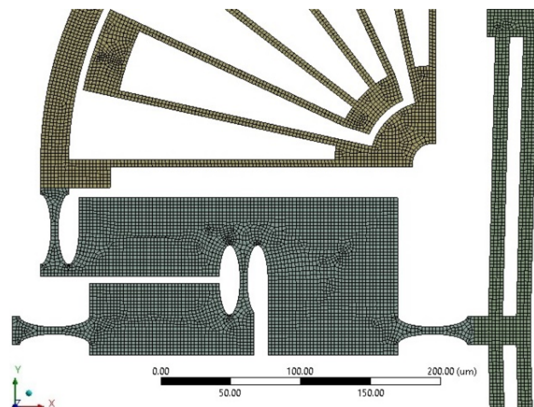

Figure 4.1: Front facing view of mesh of important components of the microgripper

4.3.1 Thermal-Electric Analysis

When electric current passes through a very thin wire, the wire heats up and its temperature increases. The heat generated is called joule heat and the phenomenon is known as Joule Heat effect. This phenomenon is used to actuate electrothermal actuators in MEMS. To study the effect of electrical power through the thin wires of chevron actuators in microgripper, this dual domain analysis is done.

After applying initial conditions, the voltage difference of 50 mV is applied at opposite ends of chevron actuator's gold layer, electric current passes through the thin wire and temperature increases. With the help of this analysis, we are able to observe the current density at any point in the gold layer and temperature at any point in microstructure.

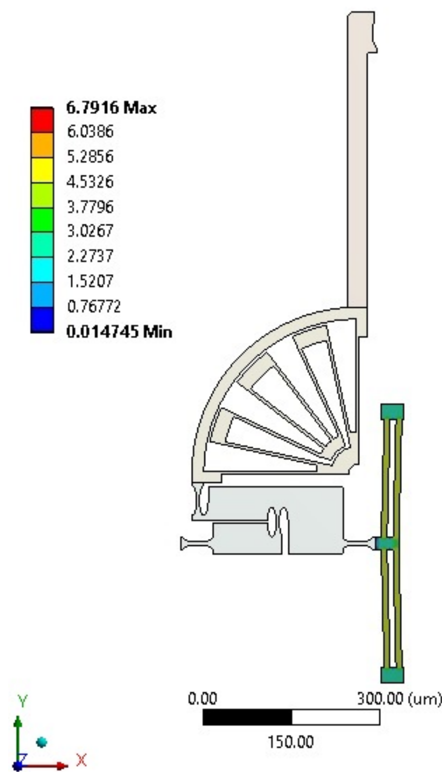

Figure 4.2: Current Density profile through gold heater in actuator

The current density profile in figure 4.2 shows uniform current density through the actuator beams. Product of cross-section of the actuator beam and current density gives value of current

through the actuator beam, which, further leads to the calculation of power consumption of complete microgripper. Compliant mechanisms and gripping jaws do not show any color as SU-8 does not conduct any electric current, shows its compatibility for biomedical applications. Maximum values of current lies at the corners near anchored points and shuttle. Current density through single actuator beam is 4.7 mA/μm^2 at 50 mV voltage.

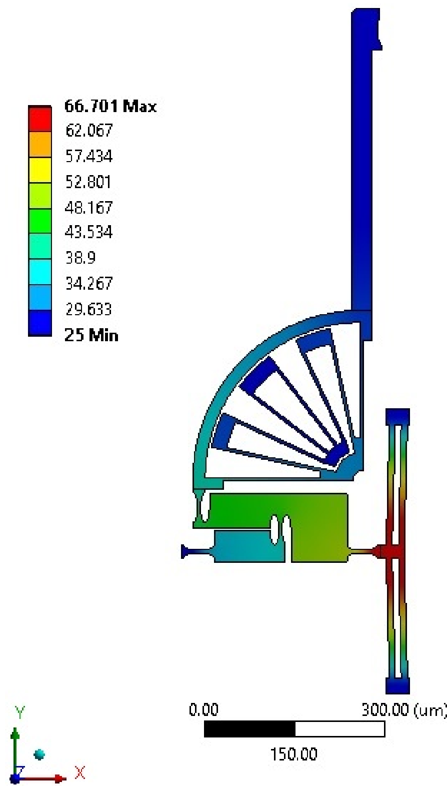

Figure 4.3: Temperature profile of complete microgripper

Temperature profile in figure 4.3 shows temperature throughout the complete microgripper. Four anchored points shows room temperature as heat sinks in to the substrate. Maximum temperature is at middle of actuators. However, some of the heat sinks to the Scott Russell mechanism and MCRF and sinks to the substrate through anchored points. The jaws of microgripper are at room temperature due to convective heat transfer to the air. Maximum temperature of 66.7 °C is at the middle of the actuator while temperature at jaw is 25 °C.

4.3.2 Static Structural Analysis

After the results from dual domain thermal electric analysis are evaluated, static structural analysis is prepared. Static structural analysis is independent from time and shows the possible physical deformations in the microstructure. This is very important for determining the performance, robustness, strength, durability and life span of the device. As the fabrication process of MEMS device are expensive and time consuming, performing this analysis saves cost of prototyping and shows if the device is prone to damage at any point.

Results from thermal electric analysis are imported in static structural analysis to visualize the effects of thermal expansion and deformation in the structure. This analysis shows if there is any displacement in each part of microgripper. Displacement leads to the occurrence of stress in torsional springs. Stress profile is used to ensure that the stress levels in the microstructure are below yield strength and does not cause any permanent damage to the microgripper.

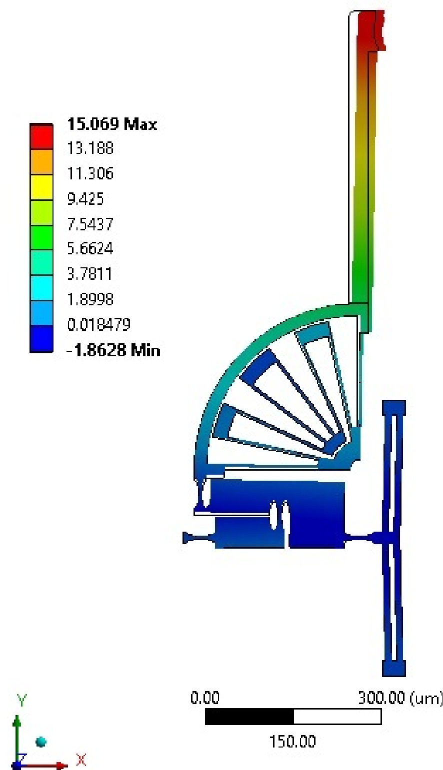

Figure 4.4: Displacement in X-axis direction

Figure 4.4 shows the displacement in X-axis direction. All the components moved in X-axis direction shows amount of displacement by respective color. Since the jaw is moving in this axis, maximum displacement can be seen at the jaw in positive X-axis. The negative value at the bottom shows the displacement at in negative X-axis which is the displacement of the actuator. Maximum displacement in X-axis direction is 15 μm.

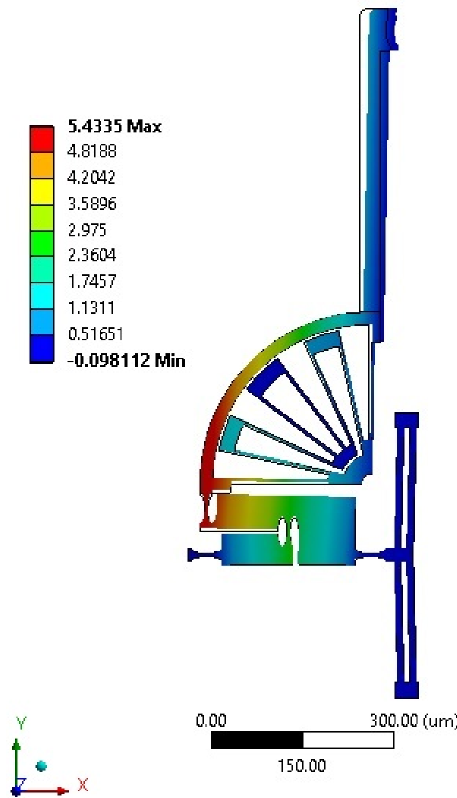

Figure 4.5: Displacement in Y-axis direction

Figure 4.5 shows the displacement in Y-axis direction. Scott Russell mechanism change the direction of displacement and force from actuator in negative X-axis direction to Y-axis direction with amplification. Maximum displacement in Y-axis direction can be observed at the junction of Scott Russell mechanism and MCRF. As the gripping arm rotates about Z-axis, very small negative Y-axis displacement is observed at the jaw. This is displacement does not effect the gripping ability and range, as the displacement is below 500 nm.

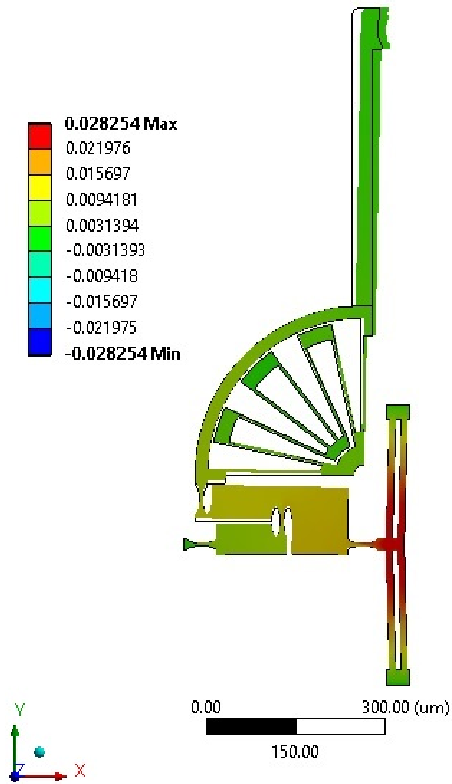

Figure 4.6: Displacement in Z-axis direction

Figure 4.6 shows displacement in Z-axis direction. Due to high coefficient of thermal expansion of SU-8, equal displacement is observed in positive and negative Z-axis direction in high temperature regions. This analysis is required to observe any out of plane motion. It is observed that there is no out of plane motion in the microstructure except due to thermal expansion which is in nanometer range.

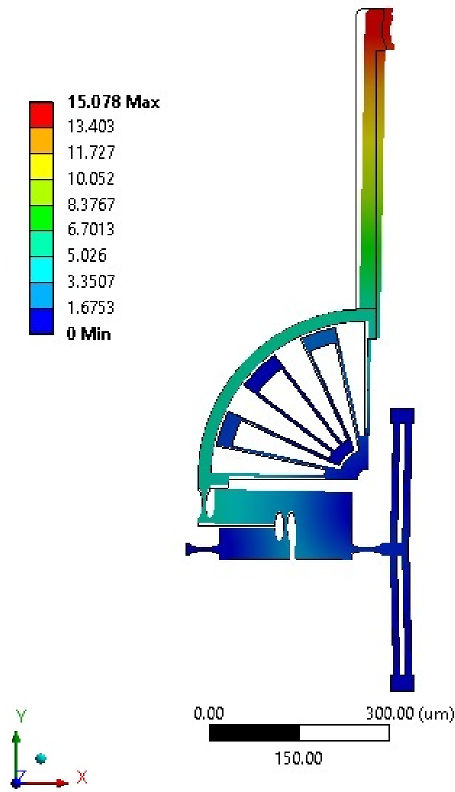

Figure 4.7: Total displacement in microgripper

Figure 4.7 shows the total displacement in the microstructure. Outer beam of MCRF shows uniform color due to its precise radial motion about the pivot. Color also shows the first amplification in displacement from Scott Russell mechanism. Maximum displacement of 15 µm is observed at the jaw, after the sencond amplification from leverage mechanism. For complete microgripper, gripping range of 62 to 92 µm is observed.

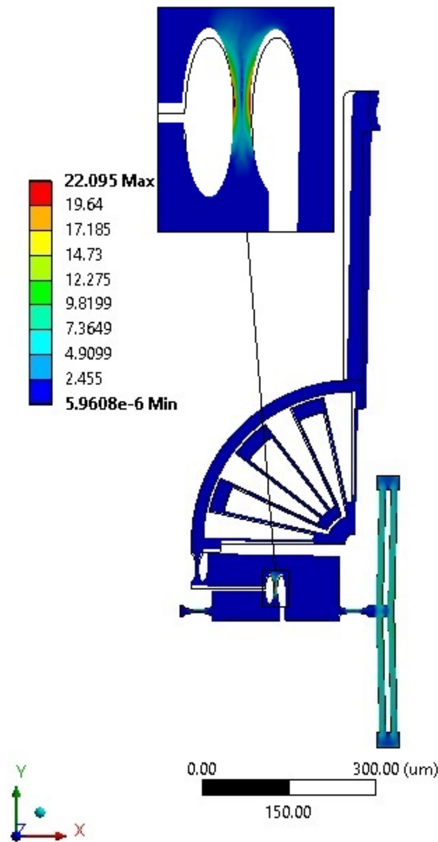

Figure 4.8: Stress profile showing maximum stress at a notch hinge

Stress profile in figure 4.8 shows the stress levels at various components of the microgripper. Maximum stress levels are observed the the edges of central notch hinge of Scott Russell mechanism. Actuator beams also showing some level of stress but not critical. MCRF is showing very low amount of stress in flexure springs, verifying that they can handle large precise rotations while keeping the stress low. Maximum stress is 22 MPa at notch hinge 'B' of Scott Russell mechanism, which is less than half of yield strength of the SU-8 material.

4.4 Results

Results are compiled from above simulations by varying the value of input voltage. Microgripper design used voltage range from 5 mV to 50 mV with the addition of 5 mV at each step. Voltage vs displacement, voltage vs change in average temperature and power vs displacement response are generated using the results from FEM simulations. These results are discussed below.

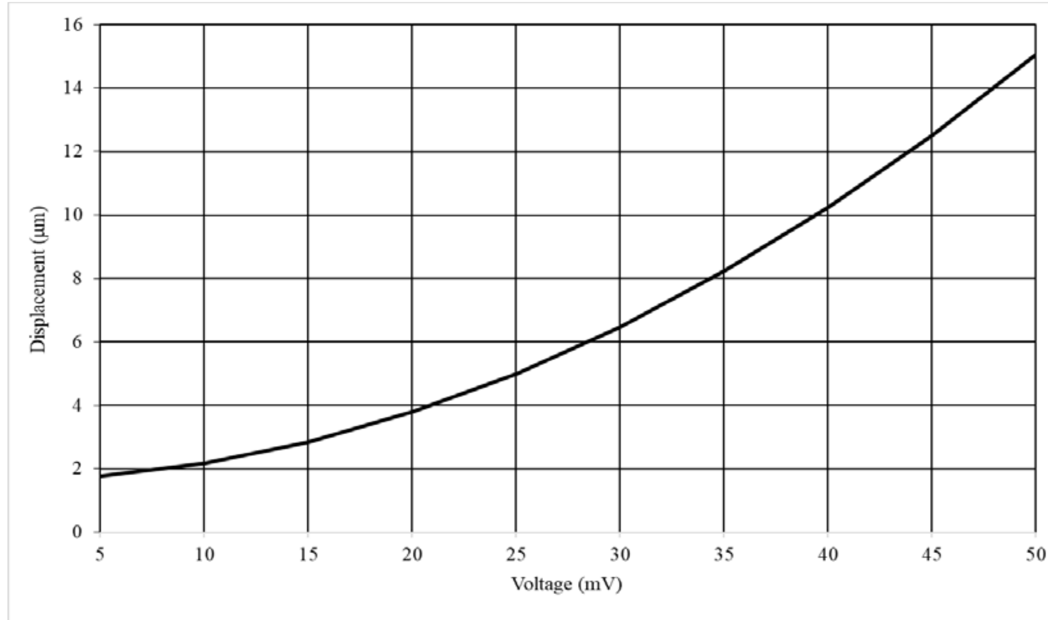

Figure 4.9: Voltage vs displacement at jaw graph from FEM

In figure 4.9, it is observed that the response of voltage vs displacement is nonlinear but close linear. Initially, with the increase in voltage, change in displacement is low. With further increase in voltage, displacement increases more than previous iteration. Displacement of 15 μm in X-axis direction is achieved at voltage of 50 mV.

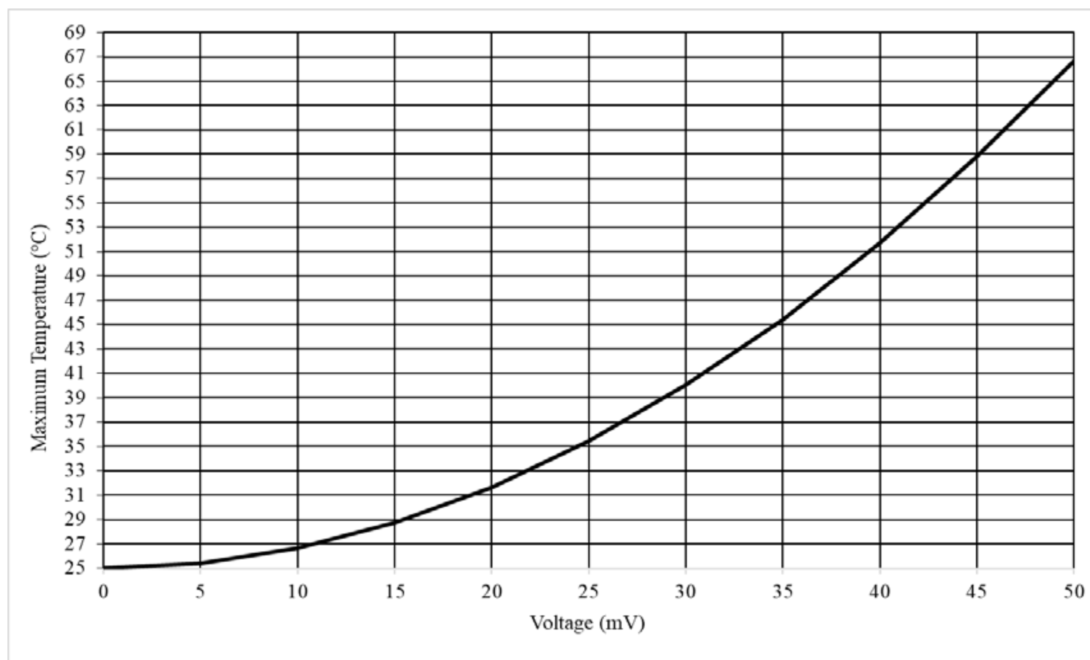

Figure 4.10: Voltage vs maximum temperature graph from FEM

Voltage vs temperature graph in figure 4.10 shows similar trends to voltage vs displacement graph. Graph shows that the displacement depends on the actuator temperature. Minimum temperature is 25 °C which is the room temperature. However, value of temperature varies with the material properties, as temperature based material properties are considered constant.

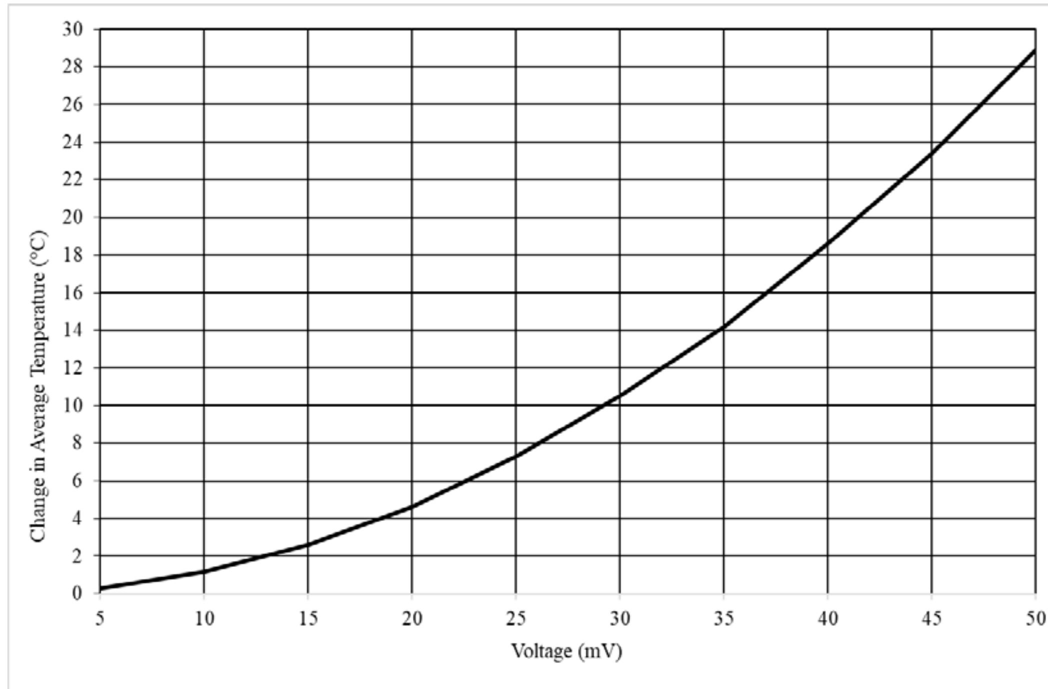

Figure 4.11: Voltage vs change in average temperature graph from FEM

Figure 4.11 shows the difference of average temperature with initial temperature in the actuator beam when a certain voltage is applied. The value of temperature determines how much the length of actuator beams increase with respect to this change in temperature. This is calculated by averaging the temperature values of all the nodes in an actuator beam and evaluating the difference with initial temperature. Maximum value of this temperature is 28.9 °C at 50 mV voltage.

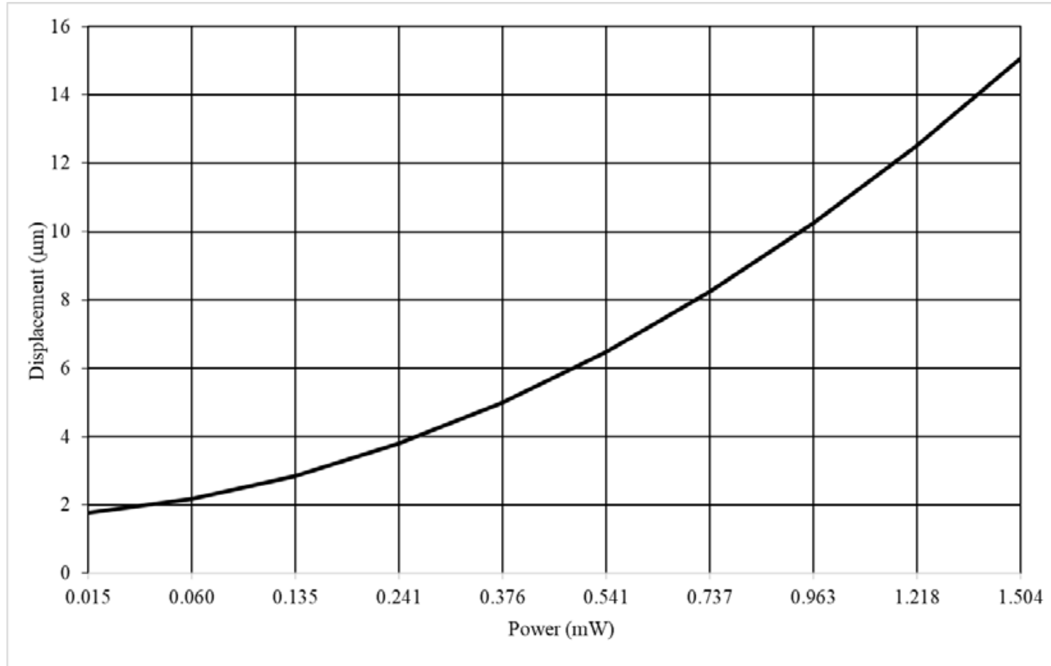

Figure 4.12: Power vs displacement at jaw graph from FEM

Similar to voltage vs displacement graph, as power is directly proportional to voltage. The graph in figure 4.12 helps to ensure minimum power consumption by the device. Graph shows nonlinear behavior. However, it is close to linear. Current is calculated by taking product of current density and cross section of gold heater at each step. Further, by taking product of voltage and current gives power. To achieve the displacement of 15 μm, 1.504 mW is required by actuator pair for single jaw of microgripper, giving it a total range of 30 μm at 3.01 mW.

In next chapter, we will verify the results of mathematical model with FEM results and compare them with other microgrippers.

CHAPTER 5: DISCUSSION AND COMPARISON

The reason behind every research is to design and make something new and better than the previous developed product. To ensure how and why a design is better than the previous designs, comparison is done between various characteristics. For a MEMS microgripper, these characteristics include cost, compatibility with multiple tasks and performance parameters. The cost of fabrication processes of a MEMS device is high. To reduce the cost of fabrication of a microgripper, low cost fabrication process and less expensive materials can be used. The reason behind using the SU-8 based fabrication process and SU-8 as a material, an epoxy based negative photoresist, is its low cost. For a microgripper compatible with biomedical applications, its ability to manipulate cells of multiple shapes and sizes without damaging them, defines its compatibility. The performance parameters are evaluated from mathematical model and FEM are compared and discussed. Comparison with other designs is also give at the end.

5.1 Mathematical Model vs FEM Results

Some of the important performance parameters of a microgripper include jaw displacement, change in average temperature, power consumption. Results compiled from mathematical model in chapter 3 and from FEM in chapter 4 are compared and discussed below.

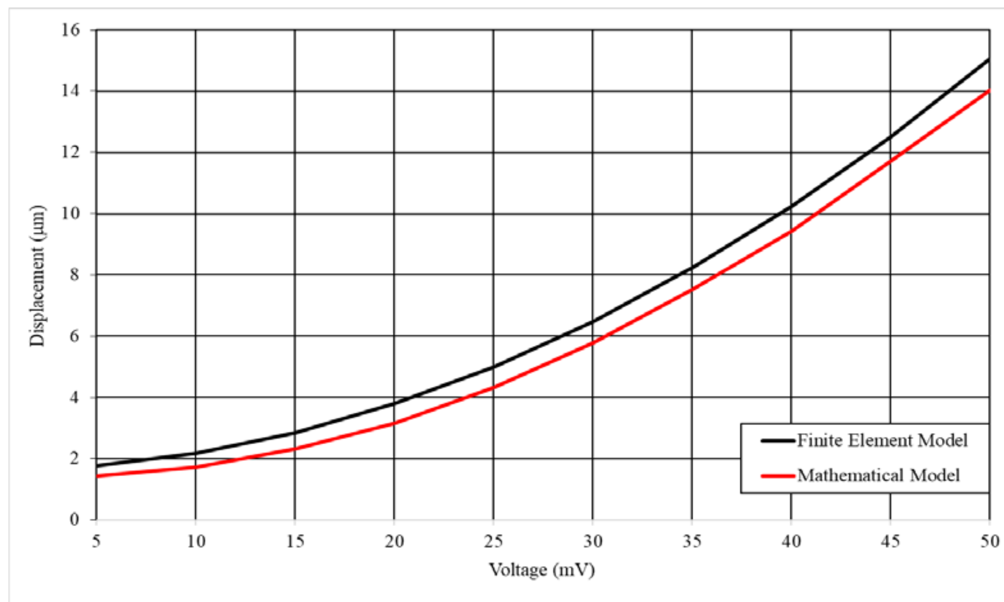

Figure 5.1: Comparison between displacement from FEM and mathematical model at the jaw

The graph in figure 5.1 is a comparison of displacement results from mathematical model and FEM simulation results. This graph shows displacement at jaw with respect to the increase in voltage. FEM simulations show slightly more displacement as compared to the mathematical model. FEM shows more displacement due the effect of temperature and heat transfer to the compliant mechanism and nonlinear amplification factor of Scott Russell mechanism. Results from both methods show nonlinear response due to nonlinear increase in temperature with respect to the input voltage.

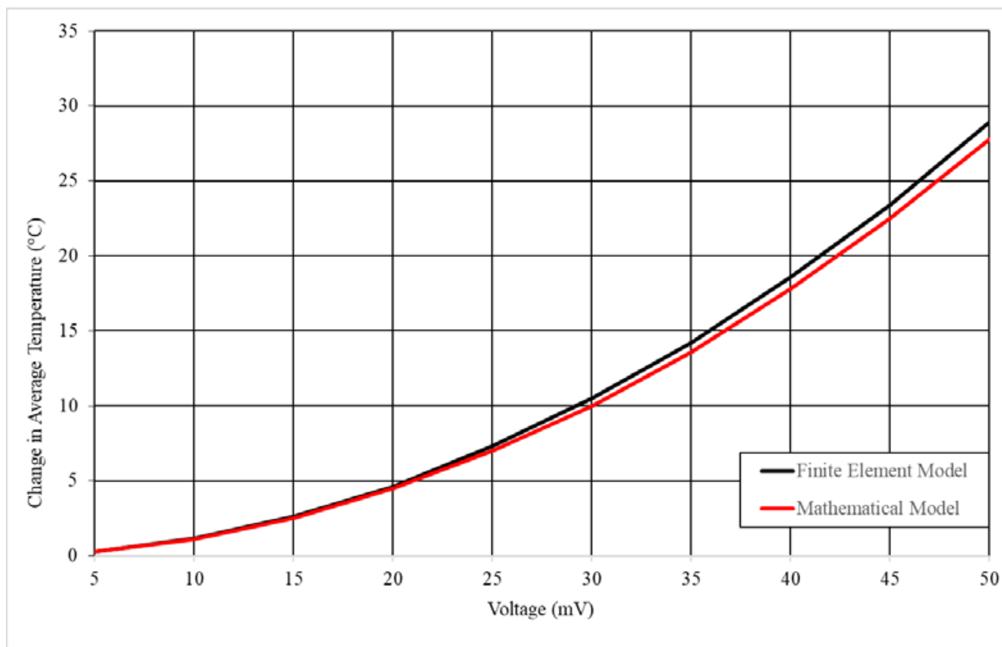

Figure 5.2: Comparison between change in average temperature from FEM and mathematical model at the jaw

In figure 5.2, graph shows response of voltage with respect to the change in average temperature from both mathematical model and FEM simulations. It is difference of initial temperature vs average value of temperature in actuator beam. As mention above, all the temperature dependent material properties are taken as constant, with the increase in voltage, the temperature in actuator beams increase in nonlinear manner. Therefore, by small increase in temperature, the temperature increases more. This behavior of electrothermal actuator benefits the microgripper in achieving large gripping ranges with small increase in voltage, after ensuring that the high temperature of actuator does not affect the gripping jaws, as the cells get damage due to high temperature. Temperature at jaws can be seen using FEM simulation to ensure the microgripper compatibility with biomedical applications. Due to low thermal conductivity of SU-

8, small amount of heat is transferred to the Scott Russell mechanism and MCRF. This causes small amount of thermal expansion in compliant mechanisms leading to additional displacement at jaws.

5.2 Discussion

The microgripper design was simulated up to 50 mV to achieve displacement of 15 µm. Simulating above 50 mV gives better displacement due to it nonlinear response, however, it increases the stress above 22 MPa at notch hinge 'B' of Scott Russell mechanism, which limits the output displacement of this design. At voltages above 50 mV, microgripper design will still work up to a certain displacement but it will reduce the life of microgripper significantly. This will make the microgripper prone to failure.

SU-8 has a low melting point of 200 °C. Gold heater in actuators have melting point higher than SU-8, so microgripper can be actuated at high temperatures. If the microgripper is actuated at temperature above 200 °C, the microstructure will be damage. For biomedical applications like cell manipulation, it is required to keep the temperature at the jaws at room temperature. Hence, low melting limits the performance of microgripper. However, at the same time, it is easier to ensure low temperature at jaws for successful bio manipulation. From FEM simulation, maximum temperature of 67 °C is at actuator beams while jaws are at room temperature.

Cells are prone to damage due to high gripping force. Compliant mechanisms used in this microgripper design provides dual displacement amplification at the gripping jaws. This large displacement amplification is to ensure the low, but suitable, gripping force up to12 µN at the jaw. Graph between external force vs displacement at jaw shows that the displacement decreases with the increase in external force at the jaws. This aids in safe gripping operation that force is not too low to lose cell under manipulation, or not too high to damage the cell between jaws.

Jaws are attached to the gripping arm of the microgripper, which also acts as a lever for leverage mechanism. Due to large gripping arm, the circular motion of the jaw has large radius and displacement of the jaw in Y-axis is small. This displacement in Y-axis direction is in nanometer range and displacement in X-axis direction is considered linear due to small rotation.

5.3 Comparison

To see the how much better the presented design is, a comparison of important characteristics of microgripper between this work and previously done work is given below. This comparison include overall size, input (power, voltage, current), output displacement and maximum temperature.

Table 5-1: Comparison between previous work and this work

Sr. #	Author	Dimensions Length × Width × Thickness (μm^3)	Input (Power, Voltage, Current)	Maximum Temperature (K)	Displacement at Jaws (μm)	Reference
1	Phan et al. 2015	490 × 110 × 30	4.5 V	543.15	32	[86]
2	Voicu et al. 2015	800 × - × 50	0.25 V	1050	20	[87]
3	Dodd et al. 2015	-	10 mA	-	20	[63]
4	Soma et al. 2017	1000 × 180 × 20	0.65 V	461	20	[69]
5	Zandi et al. 2017	760 × - × 20	0.7 V	358	11	[88]
6	This Work	1112 × 759 × 20	0.05 V@ 3.01 mW	340	30	-

CHAPTER 6: CONCLUSION

In this dissertation, a compact microgripper design with optimized performance for biomedical applications is presented. Materials for the design are selected to reduce the cost of fabrications and reduce complex process. Among various actuation methods, electrothermal actuators are used due to its compact size, large output and easily modifiable. High temperature of electrothermal actuator causes high temperature at the gripping jaws. However, with careful design and implementation of compliant mechanism reduces temperature at the jaws to room temperature. Use of compliant mechanisms in a microgripper design have multiple advantage. Compliant mechanism like leverage mechanism, Scott Russell mechanism and MCRF provides large displacement amplification, low forces at jaws, keeping the overall size compact, changing direction of motion and reduce the effect of temperature from actuator. However, if not carefully designed, compliant mechanisms might increase the size of microgripper. In compliant mechanisms, stress is low where flexure springs are used and large in size. However, stress is high where notch hinges are used and compact in size. For long operating life of the microgripper, stress is kept low to avoid any damage to microstructure. For biomedical applications and cell manipulation, jaws with wide gripping range are designed to grip variety of cells with various shapes and sizes. Low actuation voltage, low temperature and suitable force at the jaw with biocompatible material, are ensured to avoid cell damage during micromanipulation.

For future work, sensor can be implemented to detect accurate jaw motion. To make system output linear, output from sensor can be used by a dedicated control system for safe operation. To increase the gripping range of the microgripper, remove or replace the Scott Russell mechanism by a low stress mechanism with flexure springs, to reduce stress in the system and improve actuator efficiency.

REFERENCES

[1] R. Kumar, A. A. Kapoor, and R. H. Taylor, "Preliminary experiments in robot/human cooperative microinjection," in Int. Conf. Intelligent Robots and Systems (IROS 2003), vol. 3, 2003, pp. 3186–3191.

[2] A. Ashkin, "Optical trapping and manipulation of neutral particles using lasers," in Proc. Natl. Acad. Sci., vol. 94, May 1997, pp. 4853–4860.

[3] Solano, B. P., Gallant, A. J., & Wood, D. (2009, April). Design and optimisation of a microgripper: Demonstration of biomedical applications using the manipulation of oocytes. In Design, Test, Integration & Packaging of MEMS/MOEMS, 2009. MEMS/MOEMS'09. Symposium on (pp. 61-65). IEEE.

[4] Jay, J. K., Qu, H. W., Meir, S., & Lorenzo, S. (2011). Design and fabrication of electro-thermally activated micro gripper with large tip opening and holding force. In IEEE 2011 conference.

[5] Xiao, S., Li, Y., & Zhao, X. (2011, September). Optimal design of a novel micro-gripper with completely parallel movement of gripping arms. In Robotics, Automation and Mechatronics (RAM), 2011 IEEE Conference on (pp. 35-40). IEEE.

[6] Zhang, J., Lu, K., Chen, W., Jiang, J., & Chen, W. (2015). Monolithically integrated two-axis microgripper for polarization maintaining in optical fiber assembly. Review of Scientific Instruments, 86(2), 025105.

[7] Rabenorosoa, K., Clévy, C., Lutz, P., Das, A. N., Murthy, R., & Popa, D. (2009, January). Precise motion control of a piezoelectric microgripper for microspectrometer assembly. In ASME 2009 International Design Engineering Technical Conferences and Computers And Information In Engineering Conference (pp. 769-776). American Society of Mechanical Engineers.

[8] Chen, B. K., Zhang, Y., & Sun, Y. (2009). Active release of microobjects using a MEMS microgripper to overcome adhesion forces. Journal of microelectromechanical systems, 18(3), 652-659.

[9] Andersen, K. N., Carlson, K., Petersen, D. H., Mølhave, K., Eichhorn, V., Fatikow, S., & Bøggild, P. (2008). Electrothermal microgrippers for pick-and-place operations. Microelectronic Engineering, 85(5-6), 1128-1130.

[10] Zubir, M. N. M., Shirinzadeh, B., & Tian, Y. (2009). A new design of piezoelectric driven compliant-based microgripper for micromanipulation. Mechanism and Machine Theory, 44(12), 2248-2264.

[11] Chen, B. K., Zhang, Y., & Sun, Y. (2009). Active release of microobjects using a MEMS microgripper to overcome adhesion forces. Journal of microelectromechanical systems, 18(3), 652-659.

[12] Deole, U., Lumia, R., Shahinpoor, M., & Bermudez, M. (2008). Design and test of IPMC artificial muscle microgripper. Journal of Micro-Nano Mechatronics, 4(3), 95-102.

[13] Alogla, A., Scanlan, P., Shu, W. M., & Reuben, R. L. (2013). A scalable syringe-actuated microgripper for biological manipulation. Sensors and Actuators A: Physical, 202, 135-139.

[14] Yoshida, K., Tsukamoto, N., Kim, J. W., & Yokota, S. (2015). A study on a soft microgripper using MEMS-based divided electrode type flexible electro-rheological valves. Mechatronics, 29, 103-109.

[15] DESPA, V., CATANGIU, A., IVAN, I. A., GURGU, V., & ARDELEANU, M. (2014). Modeling and control of a microgripper based on electromagnetic actuation. The Scientific Bulletin of Valahia Univ, 9, 131-136.

[16] Saucedo-Flores, E., Ruelas, R., Flores, M., & Chiao, J. C. (2003). Study of the pull-in voltage for MEMS parallel plate capacitor actuators. MRS Online Proceedings Library Archive, 782.

[17] Sun, Y., Greminger, M. A., Potasek, D. P., & Nelson, B. J. (2003). A visually servoed mems manipulator. In Experimental Robotics VIII (pp. 255-264). Springer, Berlin, Heidelberg.

[18] Moore, S. I., & Moheimani, S. R. (2015). Vibration control with MEMS electrostatic drives: A self-sensing approach. IEEE Transactions on Control Systems Technology, 23(3), 1237-1244.

[19] Vineela, V., Rao, B. R., Nath, T. M., & Rao, K. S. Design and simulation of MEMS piezoelectric gyroscope.

[20] Naduvinamani, S., & Iyer, N. C. (2016, March). Design and simulation of PZT based MEMS piezoelectric accelerometer. In Electrical, Electronics, and Optimization Techniques (ICEEOT), International Conference on (pp. 3715-3721). IEEE.

[21] Duc, T. C., Lau, G. K., Creemer, J. F., & Sarro, P. M. (2008). Electrothermal microgripper with large jaw displacement and integrated force sensors. Journal of microelectromechanical systems, 17(6), 1546-1555.

[22] Pal, S., & Xie, H. (2012). Fabrication of robust electrothermal MEMS devices using aluminum–tungsten bimorphs and polyimide thermal isolation. Journal of Micromechanics and Microengineering, 22(11), 115036.

[23] Lee, J. S., Park, D. S. W., Nallani, A. K., Lee, G. S., & Lee, J. B. (2004). Sub-micron metallic electrothermal actuators. Journal of Micromechanics and Microengineering, 15(2), 322.

[24] Pala, Nezih & Nabil Abbas, Ahmad & Rockstuhl, Carsten & Menzel, Christoph & Mühlig, Stefan & Lederer, F & J. Brown, Joseph & M. Bright, Victor & Curley, Steven & Kan Koh, Yee & Pourkamali, Siavash & Heremans, Joseph & M. Chamoire, Audrey & Shankar, Karthik & Risbud, Aditi & Lakhtakia, Akhlesh & H. Bartl, Michael & Carrière, Marie & Larue, Camille & M. Rao, Apparao. (2012). Thermal Actuators. 2680-2697. 10.1007/978-90-481-9751-4_313.

[25] Shen, X., & Chen, X. (2013). Mechanical performance of a cascaded V-shaped electrothermal actuator. International Journal of Advanced Robotic Systems, 10(11), 379.

[26] Brown, J. J., & Bright, V. M. (2012). Thermal actuators. In Encyclopedia of Nanotechnology (pp. 2680-2697). Springer, Dordrecht.

[27] Zheng, X., Chen, X., Kim, J. K., & Lee, D. W. (2011). Analysis on microfinger with grooved patterns and its application in electric–thermal microgripper. The International Journal of Advanced Manufacturing Technology, 56(5-8), 505-513.

[28] Solano, B., Gallant, A. J., Greggains, G. D., Wood, D., & Herbert, M. (2008). Low voltage microgripper for single cell manipulation. In Advances in Science and Technology (Vol. 57, pp. 67-72). Trans Tech Publications.

[29] Zhang, Z., Yu, Y., Liu, X., & Zhang, X. (2015, August). A comparison model of V-and Z-shaped electrothermal microactuators. In Mechatronics and Automation (ICMA), 2015 IEEE International Conference on (pp. 1025-1030). IEEE.

[30] Voicu, R., Tibeica, C., & Muller, R. (2009, April). Design and simulation study for an electro-thermally actuated micromanipulator. In Thermal, Mechanical and Multi-Physics simulation and Experiments in Microelectronics and Microsystems, 2009. EuroSimE 2009. 10th International Conference on (pp. 1-5). IEEE.

[31] Chang, R. J., & Cheng, C. Y. (2009, July). Vision-based compliant-joint polymer force sensor integrated with microgripper for measuring gripping force. In Advanced Intelligent Mechatronics, 2009. AIM 2009. IEEE/ASME International Conference on (pp. 18-23). IEEE.

[32] Lumia, R., & Shahinpoor, M. (2008). IPMC microgripper research and development. In Journal of Physics: Conference Series (Vol. 127, No. 1, p. 012002). IOP Publishing.

[33] Yoshida, K., Tsukamoto, N., Kim, J. W., & Yokota, S. (2015). A study on a soft microgripper using MEMS-based divided electrode type flexible electro-rheological valves. Mechatronics, 29, 103-109.

[34] Alogla, A., Scanlan, P., Shu, W. M., & Reuben, R. L. (2013). A scalable syringe-actuated microgripper for biological manipulation. Sensors and Actuators A: Physical, 202, 135-139.

[35] Giouroudi, I., Hötzendorfer, H., Kosel, J., Andrijasevic, D., & Brenner, W. (2008). Development of a microgripping system for handling of microcomponents. Precision Engineering, 32(2), 148-152.

[36] Kuo, J. C., Huang, H. W., Tung, S. W., & Yang, Y. J. (2014). A hydrogel-based intravascular microgripper manipulated using magnetic fields. Sensors and Actuators A: Physical, 211, 121-130.

[37] Xu, Q. (2015). Design, fabrication, and testing of an MEMS microgripper with dual-axis force sensor. IEEE Sensors Journal, 15(10), 6017-6026.

[38] Andersen, K. N., Carlson, K., Petersen, D. H., Mølhave, K., Eichhorn, V., Fatikow, S., & Bøggild, P. (2008). Electrothermal microgrippers for pick-and-place operations. Microelectronic Engineering, 85(5-6), 1128-1130.

[39] Voicu, R., Müller, R., Eftime, L., & Tibeica, C. (2009). Design study for an electro-thermally actuator for micromanipulation. Romania. J. Inf. Sci. Technol, 12(3), 402-409.

[40] Chen, D. S., Yin, C. Y., Lai, R. J., & Tsai, J. C. (2009, January). A multiple degrees of freedom electrothermal actuator for a versatile MEMS gripper. In Micro Electro Mechanical Systems, 2009. MEMS 2009. IEEE 22nd International Conference on (pp. 1035-1038). IEEE.

[41] Colinjivadi, K. S., Lee, J. B., & Draper, R. (2008). Viable cell handling with high aspect ratio polymer chopstick gripper mounted on a nano precision manipulator. Microsystem Technologies, 14(9-11), 1627-1633.

[42] Mata, A., Fleischman, A. J., & Roy, S. (2006). Fabrication of multi-layer SU-8 microstructures. Journal of micromechanics and microengineering, 16(2), 276.

[43] Saleem, M. M., Farooq, U., Izhar, U., & Khan, U. S. (2017). Multi-response optimization of electrothermal micromirror using desirability function-based response surface methodology. Micromachines, 8(4), 107.

[44] Smith, S. T., Badami, V. G., Dale, J. S., & Xu, Y. (1997). Elliptical flexure hinges. Review of Scientific Instruments, 68(3), 1474-1483.

[45] Chen, T., Chen, L., Liu, B., Wang, J., & Li, X. (2009, January). Design of a four-arm structure MEMS gripper integrated with sidewall force sensor. In Nano/Micro Engineered and Molecular Systems, 2009. NEMS 2009. 4th IEEE International Conference on (pp. 75-79). IEEE.

[46] Chen, T., Sun, L., Chen, L., Rong, W., & Li, X. (2010). A hybrid-type electrostatically driven microgripper with an integrated vacuum tool. Sensors and Actuators A: Physical, 158(2), 320-327.

[47] Khan, F., Bazaz, S. A., & Sohail, M. (2010). Design, implementation and testing of electrostatic SOI MUMPs based microgripper. Microsystem technologies, 16(11), 1957-1965.

[48] Chang, H., Zhao, H., Xie, J., Hao, Y., Zhang, F., & Yuan, W. (2012, January). Design and fabrication of a rotary comb-actuated microgripper with high driving efficiency. In Micro Electro Mechanical Systems (MEMS), 2012 IEEE 25th International Conference on (pp. 1145-1148). IEEE.

[49] Piriyanont, B., Moheimani, S. R., & Bazaei, A. (2013, November). Design and control of a MEMS micro-gripper with integrated electro-thermal force sensor. In Control Conference (AUCC), 2013 3rd Australian (pp. 479-484). IEEE.

[50] Piriyanont, B., & Moheimani, S. R. (2014). MEMS rotary microgripper with integrated electrothermal force sensor. Journal of Microelectromechanical Systems, 23(6), 1249-1251.

[51] Hao, Y., Yuan, W., Zhang, H., Kang, H., & Chang, H. (2015). A rotary microgripper with locking function via a ratchet mechanism. Journal of Micromechanics and Microengineering, 26(1), 015008.

[52] Chang, L., Huang, X., & Wang, M. (2010, July). Research on PZT bimorph microgripper system. In Intelligent Control and Automation (WCICA), 2010 8th World Congress on (pp. 5498-5502). IEEE.

[53] Xiao, S., Li, Y., & Zhao, X. (2011, June). Design and analysis of a novel micro-gripper with completely parallel movement of gripping arms. In Industrial Electronics and Applications (ICIEA), 2011 6th IEEE Conference on (pp. 2127-2132). IEEE.

[54] Huang, H., Zhao, H., Yang, Z., Mi, J., Fan, Z., Wan, S., ... & Ma, Z. (2012). A novel driving principle by means of the parasitic motion of the microgripper and its preliminary application in the design of the linear actuator. Review of Scientific Instruments, 83(5), 055002.

[55] Sun, X., Chen, W., Tian, Y., Fatikow, S., Zhou, R., Zhang, J., & Mikczinski, M. (2013). A novel flexure-based microgripper with double amplification mechanisms for micro/nano manipulation. Review of Scientific Instruments, 84(8), 085002.

[56] Chen, W., Shi, X., Chen, W., & Zhang, J. (2013). A two degree of freedom micro-gripper with grasping and rotating functions for optical fibers assembling. Review of Scientific instruments, 84(11), 115111.

[57] Xu, Q. (2012, July). Mechanism design and analysis of a novel 2-DOF compliant modular microgripper. In Industrial Electronics and Applications (ICIEA), 2012 7th IEEE Conference on (pp. 1966-1971). IEEE.

[58] Liang, C., Wang, F., Tian, Y., Zhao, X., Zhang, H., Cui, L., ... & Ferreira, P. (2015). A novel monolithic piezoelectric actuated flexure-mechanism based wire clamp for microelectronic device packaging. Review of Scientific Instruments, 86(4), 045106.

[59] Chronis, N., & Lee, L. P. (2005). Electrothermally activated SU-8 microgripper for single cell manipulation in solution. Journal of Microelectromechanical systems, 14(4), 857-863.

[60] Voicu, R., Müller, R., Eftime, L., & Tibeica, C. (2009). Design study for an electro-thermally actuator for micromanipulation. Romania. J. Inf. Sci. Technol, 12(3), 402-409.

[61] Duc, T. C., Lau, G. K., & Sarro, P. M. (2008). Polymeric thermal microactuator with embedded silicon skeleton: Part II—Fabrication, characterization, and application for 2-DOF microgripper. Journal of Microelectromechanical Systems, 17(4), 823-831.

[62] Solano, B., Merrell, J., Gallant, A., & Wood, D. (2014). Modelling and experimental verification of heat dissipation mechanisms in an SU-8 electrothermal microgripper. Microelectronic Engineering, 124, 90-93.

[63] Dodd, L. E., Ward, S. C., Cooke, M. D., & Wood, D. (2015). The static and dynamic response of SU-8 electrothermal microgrippers of varying thickness. Microelectronic Engineering, 145, 82-85.

[64] Mackay, R. E., Le, H. R., & Keatch, R. P. (2011). Design optimisation and fabrication of SU-8 based electro-thermal micro-grippers. Journal of Micro-Nano Mechatronics, 6(1-2), 13-22.

[65] Mackay, R. E., Le, H. R., Clark, S., & Williams, J. A. (2012). Polymer micro-grippers with an integrated force sensor for biological manipulation. Journal of micromechanics and microengineering, 23(1), 015005.

[66] Zhang, R., Chu, J. K., & Chen, Z. P. (2011, June). A novel SU-8 electrothermal microgripper based on type synthesis of kinematic chain method. In Solid-State Sensors, Actuators and Microsystems Conference (TRANSDUCERS), 2011 16th International (pp. 466-469). IEEE.

[67] Chu, J., Zhang, R., & Chen, Z. (2011). A novel SU-8 electrothermal microgripper based on the type synthesis of the kinematic chain method and the stiffness matrix method. Journal of Micromechanics and Microengineering, 21(5), 054030.

[68] Voicu, R., & Muller, R. (2013, April). New electro-thermally actuated micromanipulator with optimized design and FEM simulations analyses. In Design, Test, Integration and Packaging of MEMS/MOEMS (DTIP), 2013 Symposium on (pp. 1-6). IEEE.

[69] Somà, A., Iamoni, S., Voicu, R., Müller, R., Al-Zandi, M. H., & Wang, C. (2018). Design and experimental testing of an electro-thermal microgripper for cell manipulation. Microsystem Technologies, 24(2), 1053-1060.

[70] Kim, K., Liu, X., Zhang, Y., & Sun, Y. (2008). Nanonewton force-controlled manipulation of biological cells using a monolithic MEMS microgripper with two-axis force feedback. Journal of Micromechanics and Microengineering, 18(5), 055013.

[71] Kim, K., Liu, X., Zhang, Y., Cheng, J., Wu, X. Y., & Sun, Y. (2009). Elastic and viscoelastic characterization of microcapsules for drug delivery using a force-feedback MEMS microgripper. Biomedical Microdevices, 11(2), 421.

[72] Huang, S. C., & Lin, D. Y. (2008, June). Optimal Design of a Closed-Loop Control Compliant Microgripper. In Innovative Computing Information and Control, 2008. ICICIC'08. 3rd International Conference on (pp. 523-523). IEEE.

[73] Huang, S. C., & Chen, W. L. (2008, October). Design of topologically optimal microgripper. In Systems, Man and Cybernetics, 2008. SMC 2008. IEEE International Conference on (pp. 1694-1698). IEEE.

[74] Huang, S. C., Chiu, C. C., & Chen, W. L. (2009). Design and fabrication of a microgripper with a topology optimal compliant mechanism. International Journal of Computational Materials Science and Surface Engineering, 2(3-4), 282-301.

[75] Hoxhold, B., & Büttgenbach, S. (2010). Easily manageable, electrothermally actuated silicon micro gripper. Microsystem Technologies, 16(8-9), 1609-1617.

[76] Ali, N., Shakoor, R. I., & Hassan, M. M. (2011, December). Design, modeling and simulation of electrothermally actuated microgripper with integrated capacitive contact sensor. In Multitopic Conference (INMIC), 2011 IEEE 14th International (pp. 201-206). IEEE.

[77] Demaghsi, H., Mirzajani, H., & Ghavifekr, H. B. (2014). Design and simulation of a novel metallic microgripper using vibration to release nano objects actively. Microsystem technologies, 20(1), 65-72.

[78] Pasumarthy, A., Dwivedi, A. K., & Islam, A. (2015, January). Optimized design of Au-polysilicon electrothermal microgripper for handling micro objects. In international conference on electrical, electronics, signals, communication and optimization (EESCO) (pp. 1-5).

[79] Shivhare, P., Uma, G., & Umapathy, M. (2016). Design enhancement of a chevron electrothermally actuated microgripper for improved gripping performance. Microsystem Technologies, 22(11), 2623-2631.

[80] Yang, S., & Xu, Q. (2016). Design of a microelectromechanical systems microgripper with integrated electrothermal actuator and force sensor. International Journal of Advanced Robotic Systems, 13(5), 1729881416663375.

[81] Margarita, T. T., Pedroa, V. C., Svetlanaa, K., Ramóna, C. R., Alejandraa, O. D., & Gerardoa, V. D. (2016). Design and simulation of a MEM microgripper based on electrothermal microactuators. In Proc. of SPIE Vol (Vol. 9936, pp. 99360I-1).

[82] Chen, C. M., Hsu, Y. C., & Fung, R. F. (2012). System identification of a Scott–Russell amplifying mechanism with offset driven by a piezoelectric actuator. Applied Mathematical Modelling, 36(6), 2788-2802.

[83] Xu, Q. (2017). Design and implementation of large-range compliant micropositioning systems. John Wiley & Sons.

[84] Iamoni, S., & Somà, A. (2014). Design of an electro-thermally actuated cell microgripper. Microsystem technologies, 20(4-5), 869-877.

[85] Zhang, Z., Zhang, W., Wu, Q., Yu, Y., Liu, X., & Zhang, X. (2016). Closed-form modelling and design analysis of V-and Z-shaped electrothermal microactuators. Journal of Micromechanics and Microengineering, 27(1), 015023.

[86] Phan, H. P., Nguyen, M. N., Nguyen, N. V., & Chu, D. T. (2017). Analytical modeling of a silicon-polymer electrothermal microactuator. Microsystem Technologies, 23(1), 101-111.

[87] Voicu, R. C., & Műller, R. (2014). Design and FEM analysis of a new micromachined electro-thermally actuated micromanipulator. Analog Integrated Circuits and Signal Processing, 78(2), 313-321.

[88] Al-Zandi, M. H., Wang, C., Voicu, R., & Muller, R. (2018). Measurement and characterisation of displacement and temperature of polymer based electrothermal microgrippers. Microsystem Technologies, 24(1), 379-387.

Completion Certificate

It is to certify that the thesis titled "Design of an Electrothermally Actuated SU-8 based Microgripper for Biomedical Applications" submitted by registration no.00000119954, NS Muhammad Zaeem Abbas of MS-86 Mechatronics Engineering is complete in all respects as per the requirements of Main Office, NUST (Exam branch).

Supervisor: _____________
Dr. Muhammad Mubasher Saleem

Date: ____ July, 2018